Author
EWELIKE, Edward O.

PG/M.Sc/87/5642

Title
Archaeological Investigations In Ogbodu-Aba (Isi-Uzo Local Government Area, Anambra State) Using Electrical Resistivity Methods

Faculty
Physical Sciences

Department
Geology

Date
February, 1990

ARCHAEOLOGICAL INVESTIGATIONS IN OGBODU-ABA (ISI-UZO LOCAL GOVERNMENT AREA, ANAMBRA STATE) USING ELECTRICAL RESISTIVITY METHODS.

EWELIKE, EDWARD OBIECHEFU
B.Sc (Hons) Geology and Mining
(PG/M.Sc/87/5642)

PROJECT REPORT SUBMITTED TO THE DEPARTMENT OF GEOLOGY IN THE FACULTY OF PHYSICAL SCIENCES IN PARTIAL FULFILMENT OF THE REQUIREMENTS FOR THE DEGREE OF MASTER OF SCIENCE (APPLIED GEOPHYSICS).

UNIVERSITY OF NIGERIA, NSUKKA

CERTIFICATION

Mr. EWELIKE, Edward Obiechefu, a Postgraduate student in the Department of Geology, University of Nigeria, Nsukka has satisfactorily completed the requirements for the award of the degree of Master of Science (Apllied Geophysics) in the Department of Geology.

The work embodied in this Project Report is original and has not been submitted in part or full for any other diploma or degree of this or any other University.

Dr. K.M. Onuoha
Supervisor
Geology Department
U.N.N.

Head of Department,
Geology Department
U.N.N.

DEDICATION

Most humbly dedicated to my beloved mother Mrs. Christiana Adaure Ewelike, for what she has been to me.

TABLE OF CONTENTS

CONTENTS (CONTD.)

LIST OF TABLES

LIST OF FIGURES

FIGURE

LIST OF FIGURES (CONTD.)

FIGURE

ACKNOWLEDGEMENT

To my supervisor, Dr. K. M. Onuoha for his intelligent criticisms and suggestions and yet for his innate love and kindness to students which remain an examplary virtue to humanity;

To Mr. and Mrs J. Nwokoro for their deeply appreciated benevolence in taking over the onerous task of fanning the embers of financial sponsorship;

To my mother, Mrs. Christiana Adaure Ewelike for her unyielding love and care amidst deprivations and sufferings in the course of my education;

To my friends and colleagues: Tony Nwonwu, Emeka Ezeajuh, Pat Okoye, and a host of others for their exciting companionship and warm encouragemtnts;

To my brothers and sisters especially Chinedu Ewelike and Catherine Ewelike for their care, understanding and patience;

To all who have recognized and appreciated the value of my endeavour.

ABSTRACT

Electrical resistivity profiling was conducted around Ogbodu-Aba to locate suspected subsurface cavities of archaeological interest. The method employed was the Wenner electrode system and the tripotential technique, which involved measuring 3 resistances (at a station) corresponding to three different electrode arrangements: CPPC, CCPP and CPCP. The resistances were designated as R^{α} , R^{β} and R^{γ} and the calculated apparent resistivities denoted as ρ^{α} , ρ^{β} and ρ^{γ} respectively.

Plots of ρ^{α} and ρ^{γ} against midpoints were made for every traverse, while a third plot; the percentage residual resistivity ($\rho^{\alpha} - \rho^{\beta} - \rho^{\gamma} \times \frac{100}{\rho^{\alpha}}$) against midpoints was also made for each traverse. The diagrams were studied and after due considerations, eight anomalous zones were delineated. Based on available, relevant geological and archaeological information, the anomalies were attributed to the possible presence of hollow cavities (ancient burial sites) in the subsurface. The sizes and depths of burial of the identified cavities ranged from 1.5 to 6m and 0.55 to 1.5m respectively.

CHAPTER ONE

INTRODUCTION

1.1 Background Archaeological information on the area

According to Chikwendu (1980), in November, 1979, the Cimeco Engineering Company was constructing a road which passed through Ogbodu-Aba. In the process of levelling a small hill to reduce the gradient, the bulldozers exposed some subterranean cavities which were found to contain human skulls in pottery bowls. The report came to the notice of some experts at the Archaeology Department of the University of Nigeria. On reaching the site, they discovered that what was being exposed and destroyed were catacombs in which important personalities of a prehistoric community were buried. They, then, mounted a rescue excavation to salvage materials which the bull-dozers had not yet destroyed.

During further excavation, it was discovered that the burial chambers were sited inside a compact laterite horizon underneath a clayey-loamy top soil. Six chambers were opened during the initial excavation. A typical chamber had a cone shaped shaft, at the base of which was an ovoid-shaped chamber.

Chikwendu (1980) noted that the builders of the chambers first of all sunk a hole through the top soil. On reaching the lateritic layers, the hole was widened and continued downwards for about 1.5 to 2 metres. From this point, the chamber itself was made tangential to the original shaft so that on completion, it looked like a Weaver bird's nest. The cavity was then compacted further by malletting and the entire structure then smoked to dessicate it. Evidence for the smoking was provided by the presence of soot inside the chambers and by the enormous ash and charcoal heaps outside the chambers. Each chamber was connected to the other by a labyrinth of underground tunnels. After the body was buried, the tunnel was closed with wet laterite and the vertical shaft covered with a big lateritic stone.

Of much interest were the types of materials recovered from the chambers. Prominent among these were human skulls found in pottery bowls and remnants of the bones and feet. Almost all the burial chambers contained an assortment of grave-goods, all made of iron. These included crotal-like implements, barbed spear heads, axes, adze-like implements and iron spira coils.

The excavated chambers described above and the artefacts recovered from them were all on that portion of the hill disturbed by the road construction. On the right side of this road was another portion of the hill yet undisturbed by the construction. However, a few of the cavities already exposed extended into this undisturbed zone. The archaeologists suspected that a good number of these burial chambers may be present within this undisturbed zone. A few excavations were later made on this zone and similar cavities and materials were discovered.

The entire area is currently of immense archaeological importance and interest. Chikwendu (1980) noted that the people who constructed the Ogbodu-Aba chambers were ingenious. The choice of site, the method of the construction, the pains taken to dessicate the chambers to enhance preservation, the elaborate mortuary items - all point to an industrious and intelligent prehistoric community. He has also highlighted the tourist potentials of the area. The archaeologists hope to open some of the burial chambers in the undisturbed portion of the hill, and organize them into a tourist centre. They hope that the public would visit the site with a view to reviving this mode of burial, which is not only traditional, but also very dignified. However, before this could be achieved, a proper delineation of the subsurface cavities is required. This, would then facilitate the excavation. Such proper delineation calls for the introduction of geophysical methods for the precise location of the subsurface cavities of interest.

1.2 Objectives of the present study

The major objective of this work was to delineate underground burial cavities within the undisturbed portion of the Asaba hill in Ogbodu-Aba using the electrical resistivity method. It is expected that a successful delineation of these cavities would assist the archaeologists in their excavations and thus contribute to meeting their ultimate goal in the entire archaeological venture.

The work involved horizontal resistivity profiling using the tripotential technique, computation of resistivity values from measured resistances, presentation of data in plots and identification and interpretation of anomalous zones and discussion of the results in terms of their archaeological sighificance.

1.3 Location of the Area

The studied area is located on the north-eastern part of

Asaba village in Ogbodu-Aba in Isu-Uzo local Government Area of Anambra State. The site is to be found to the right along Ogbodu-Aba - Akpoga road at approximately half a kilometer from Ogbodu-Aba market. Figure 1 gives the accessibility details.

The studied portion of the hill measures about 90 x 45m thus covering an area of about $4050m^2$. The work involved close resistivity measurements for archaeological purposes along traverses at very close intervals and with electrode spacing as small as 3m along traverses a few metres apart.

The Ogbodu-Aba - Akpoga road forms the northern boundary of the site. Three pathways (leading to houses located on the hill) also cut across the study area from the Ogbodu Aba - Akpoga road. At least three houses stand within the survey premises which are devoted mainly to farming by the owners of the land.

1.4 The Geology of the Area

In this area loamy topsoil constitutes the over-burden and the target of the survey. This over-burden is as thick as 3m and rests on shaly layers. This was the dominant lithology observed throughout the hill. Sometimes the over-burden

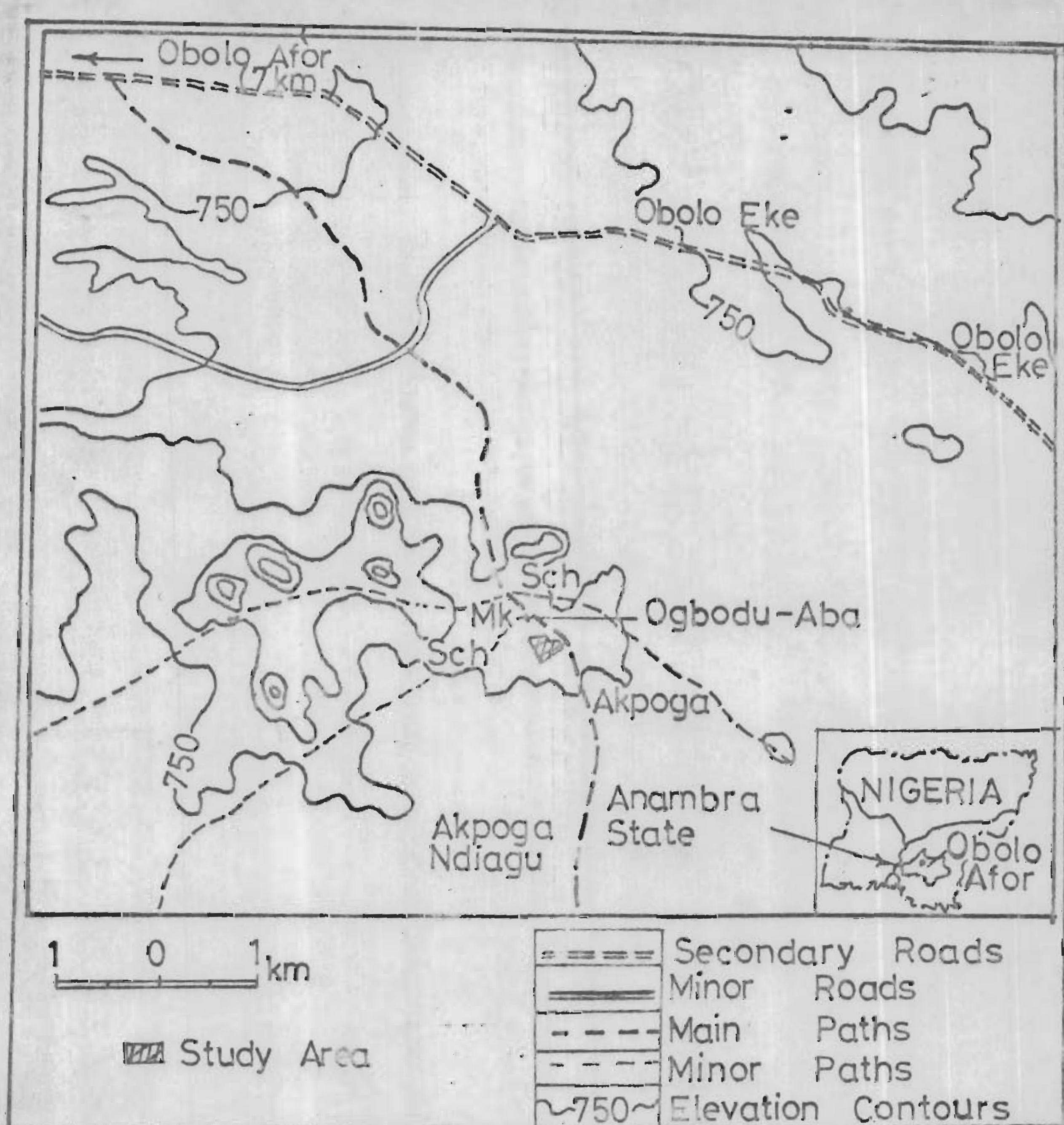

Fig. 1: Sketch Map Showing the Location of the Study Area.

rests directly on clayey layers. The thickness of this over-burden increases at the northern portion of the hill where alternating layers of shale/clay and sandstone could be observed clearly along the slops. A spring occurrs along one of the clay/sandstone boundaries at approximately 14 metres from the top of the hill. This roughly agrees with the depth to the water table (15m) measure in a well dug in the survey area.

The loamy topsoil overlying shaly or clayey layers also constitutes the dominant lithology observed within the entire Ogbodu Aba. Sands and gravels were also seen along slopes and sometimes at the foot of hills.

The entire region lies within the Nsukka Formation which is a major geoleogical formation found in the lower Benue trough. It consists of alternations of sandstones (sometimes cross bedded), shales and thin coal seams. At the top of the sequence, thin sequences of limestones occur. Table 1 shows the position of the Nsukka Formation within the Cretaceous and Tertiary sequences of South-eastern Nigeria.

The formation has been given different ages by different authors. An age of Maestrichtian to Palaeocene has been assigned to it. The formation was deposited under paralic conditions which prevailed during the second post-Santonion transgressive cycle.

Table 1: Cretaceous and Tertiary Sequence in South Eastern Nigeria

	Recent	Marine deltaic deposits
Neogene	Miocene-Pliocene	Benin Formations
	Oligocene-Miocene	Ogwashi-Asaba Formation
	Ludian	Not represented
	Bartonian	Possibly upper part of Ameki Formation
	Lutetian	Ameki Formation
	Ypressian	Possibly part ·Nanka
		of Ameki Formation Sand
	Paleocene	Imo Shale
	Danian	Nsukka Formation
		Ajali Sandstone
	Maestrichtian	Mamu Formation
	Campanian	Enugu Nkporo Shale
	Coniacian-Santorian	Shale Awgu Shale
	Turonian	Eze-Aku Shale
	Cenomanian	Odukpani Formation
Lower Cretaceous	Albian	Unnamed Formation Abakaliki Asu River Shale Group

1.5 A Review of the Use of Electrical Methods in Archaeological Investigations

Electrical resistivity profiling has been in use for over 60 years but its application to archaeological exploration, especially in the detection of cavities has received limited coverage in the literature.

Wynn (1986) reviewed the geophysical methods used in archaelogical prospecting and pointed out that the resistivity measurements were very useful in supplying information about the subsurface content of archaeological sites especially in the location of buried ditches, stone foundations, burial holes and cavities.

McDowell (1975) pointed out that the success of any particular geophysical method for locating filled sink holes and other buried cavities depended upon the contrast in the appropriate physical properties of the infill and the host material. According to McCann et al (1987), there is the need to investigate the background noise within the survey area before the actual field measurement. The background noise refers to the influence of near surface irregularities on the resistivity readings. This background noise, if not properly studied, may mask the resistivity anomalies that could be produced by the archaeological features. They can also introduce distortions on the recorded resistivity readings. This is particularly important when the archaeological features being searched occur within shallow depths.

Maxwell (1976) found out that a void would just be detectable by the electrical profiling method if the depth of cover was less than the radius of the void. This view is also in line with an earlier study by Van Nostrand (1953) who showed that a spherical cavity with depth more than the width cannot be detected by conventional resistivity systems. According to Habberjam (1969) and McCann et al (1987), for a spherical cavity to be detected, the radius should be less than or equal to electrode spacing and the electrode spacing should be less than twice the radius.

McCann et al (1987) have also discussed two electrical surveying techniques that are suited to the detection of cavities. These include systems with limited depth of investigation used for near-surface lateral variations and systems with specialized electrode arrays for greater depths of investigation and better resolution. They showed that cavities have a higher resistivity than host rock when air filled and a lower resistivity when water or sediment filled.

Earlier workers had actually used different measuring arrangements for detecting cavities. Palmer (1954) used a Wenner sounding to show the effects of an air-filled cavity. Love (1966) used Wenner soundings and fixed-separation Wenner traverses over solution cavities and sink holes along a highway route and was able to detect likely cavities using traversing rather than expanding soundings. McDowell (1975) and Greenfield (1979) were able to detect a clay filled sink hole and an air-filled cave respectively using constant separation traversing. Bristow (1966) used a pole-dipole method and graphical constructions to indicate the position of an air filled cavity. Owen and Suhler (1980) successfully detected voids in limestones using a modification of Bristow's method. Kunetz (1966) has used what he called a gradient array or rectangle method of electrode arrangement and has shown that this provided greater resolution and depth of investigation than the ordinary Wenner array.

The above methods have met with success in many cases. However, one method, the tripotential resistivity method provides extra advantage of checking instrumental error. This method was introduced by Roman (1931) and reviewed by Carpenter (1955), Carpenter and Haberjam (1956). Sarma (1961) studied a modified tripotential prospecting method. The actual application of this method to detection of spherical cavities was done by Haberjam (1969) who identified two parameters derivable from the plots and which could be used for estimating the sizes and depths of burial of cavities. Kirk (1977) pointed out the usefulness of what he called "percentage residual resistivity" in tripotential surveys in detecting the location, surface width and approximate minimum depth of fracture zones (also applicable to cavities) especially in shale - sandstone terrains.

CHAPTER TWO

DATA ACQUISITION

The Geophysical method employed in this survey was the electical resistivity system employing the Wenner tripotential technique. The basic principles of the electrical resistivity method, the Wenner system and the tripotential techniques are described in this chapter.

2.1 Basic Principles of the Electrical Resistivity Method

The electrical resistivity method utilizes the concept of electric current flow in the ground. The basis of this is Ohm's Law which states that

$$V = IR \quad \ldots\ldots\ldots\ldots\ldots \quad (1)$$

V = Potential difference between any two points

I = Current flowing in the conducting medium

R = Resistance of the medium between these two points.

The resistivity, ρ, of the material is defined as the resistance across a unit cube of the material. So if current is flowing between two points of a conductor of cross-sectional area A, a distance apart, then the resistance between these two points is given by the formula:

$$R = \frac{\rho d}{A} \quad \ldots\ldots\ldots\ldots\ldots \quad (2)$$

Parasnis (1966) has shown that if I is the current passing through a point electrode, placed on a flat semi-infinite earth of resistivity ρ , the electric potential at a point P, a distance d, from the electrode is:

$$V = \frac{I\rho}{2\pi d} \quad \ldots\ldots\ldots\ldots\ldots \quad (3)$$

In the resistivity method, and electric current is introduced into the ground by means of two current electrodes and the potential difference between two potential electrodes is measured. The simplest method of conducting a resistivity survey is to arrange the four electrodes in a straight line on the surface of the ground. This is shown in Figure 2 below.

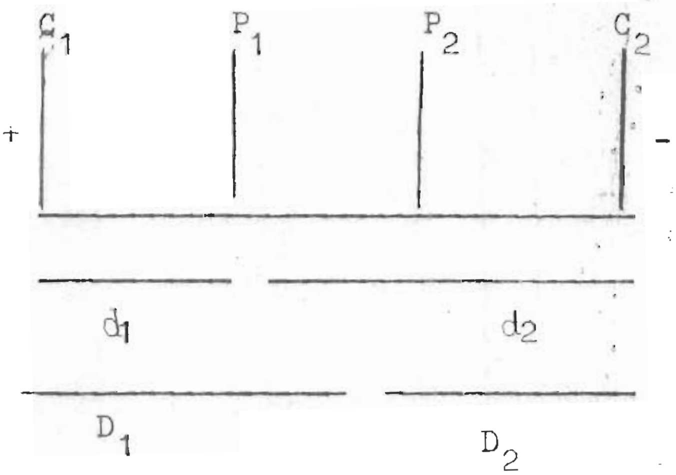

Fig. 2: The Four electrode array in resistivity prospecting (vingoe 1972)

From the above diagram it can be shown that

$$V_{P_1} = \frac{I\rho}{2\pi} \left(\frac{1}{d_1} - \frac{1}{d_2} \right) \text{ and}$$

$$V_{P_2} = \frac{I\rho}{2\pi} \left(\frac{1}{D_1} \quad \frac{1}{D_2} \right).$$

Therefore the potential difference between points P_1 and P_2 is:

$$V_{P_1} - V_{P_2} = V = \frac{I\rho}{2\pi} \left(\frac{1}{d_1} - \frac{1}{d_2} - \frac{1}{D_1} + \frac{1}{D_2} \right.$$

Therefore the resistivity becomes:

$$\rho = \frac{2\pi \ \Delta V}{I} \left(\frac{1}{\frac{1}{d_1} - \frac{1}{d_2} - \frac{1}{D_1} + \frac{1}{D_2}} \right) \ \ldots\ldots \ (4)$$

$$\text{OR } \rho = 2\pi K \frac{\Delta V}{I} \ \ldots\ldots\ldots\ldots\ldots\ldots\ldots\ldots \ (5)$$

In equation 5, K replaced the whole expression in paranthesis in equation 4. It is termed the geometrical factor and is calculated from the appropriate distances between the electrodes.

On inhomogenous ground the resistivity (ρ) changes if the electrode configuration is altered or moved to a new location. Therefore, on inhomogenous ground, the value of ρ obtained from equation 5 on inserting the appropriate quantities is known as the apparent resistivity, and is usually denoted by ρa. ρa is equivalent to the true resistivity of the ground only when the ground is homogenous.

2.2 The Wenner Arrangement

In actual practice a number of different surface configurations are used for the current and potential electrodes. The current electrodes are generally placed on the outside of the potential electrodes, although the opposite arrangement should be equivalent in principle.

One of the most widely used configurations is the Wenner electrode configuration. This is illustrated in Figure 3 below.

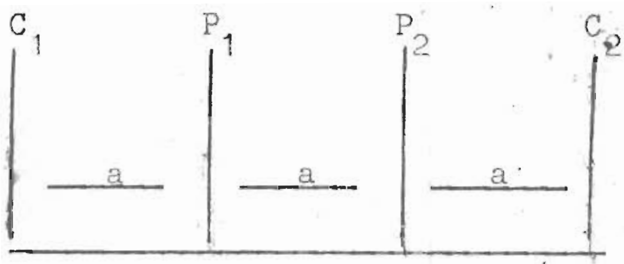

Fig. 3: The Wenner electrode configuration (Dobrin 1976).

The electrode separations (a) are equal. Using equation 4, the apparent resistivity (ρa) becomes:

$$a = \frac{2\pi\Delta V}{I}\left(\frac{1}{\frac{1}{a} - \frac{1}{2a} - \frac{1}{2a} + \frac{1}{a}}\right)$$

$$= 2\pi a \frac{\Delta V}{I}$$

The Wenner electrode system is used for depth probing and also for lateral resistivity investigation. In the former, the configuration centre is fixed but the separation of the electrodes is progressively increased. In lateral resistivity investigation, the electrode separations are fixed, and the array of electrodes is moved laterally along a profile with constant separation. The calculated apparent resistivity values are plotted against the midpoints of the configuration. The behaviour of the plot is studied and anomalies are picked and interpreted, sometimes using resistivity modelling. From this, the source of the anomalies are deduced and their sizes and depths calculated.

The Wenner electrode system has been used successfully in detecting subsurfaace features. The type of field procedure depends on the objective of the survey. For the detection of cavities suspected in an area, the lateral resistivity profiling is ideal. This has been described briefly in section 2.2. Love (1966), McDowell (1975) and Greenfield (1979) have successfully used this method in locating filled sink holes. Fixed-separation Wenner traverses were run over the suspected areas. The sizes of the cavities and depth of investigation (depth of burial of the cavities) determined the electrode spacing.

In Wenner array, the depth of investigation is approximately the same as the electrode separation. The sizes of the cavities also determine the distance bewtween the measured stations and intervals between the traverses.

The interpretation of anomalies obtained in Wenner electrode traversing may involve complex mathematical modelling. In this case the cavities are regarded as spheres; insulating spheres when they contain conductive materials (eg. Clays).

The ability of the ordinary Wenner system in delineating subsurface cavities cannot be over-emphasized. However certain problems and limitations abound. An example may be the complex mathematical modelling involved in the interpretation of anomalies.

To avoid this approach we require some slight modification in the Conventional Wenner. We also would like to achieve better resolution and avoid instrumental errors. One method for achieving this is to use the wenner Tripotential Resistivity approach which is described in greater detail below.

2.2 The Wenner Tripotential Resistivity Method

The tripotential method of resistivity prospecting could be described as follows: In a four electrode configuration, all the four electrodes can be connected in three differant manners to get different values of resistivity at a measuring point. These principal methods of connecting the four electrodes to a current source (c) and a potential measuring device (p) are, CPPC, CCPP and CPCP and will be designated respectively as the α, β and γ configurations with the corresponding apparent resistivities: ρ^{α}, ρ^{β} and ρ^{γ} .

Figure 4 shows the configurations.

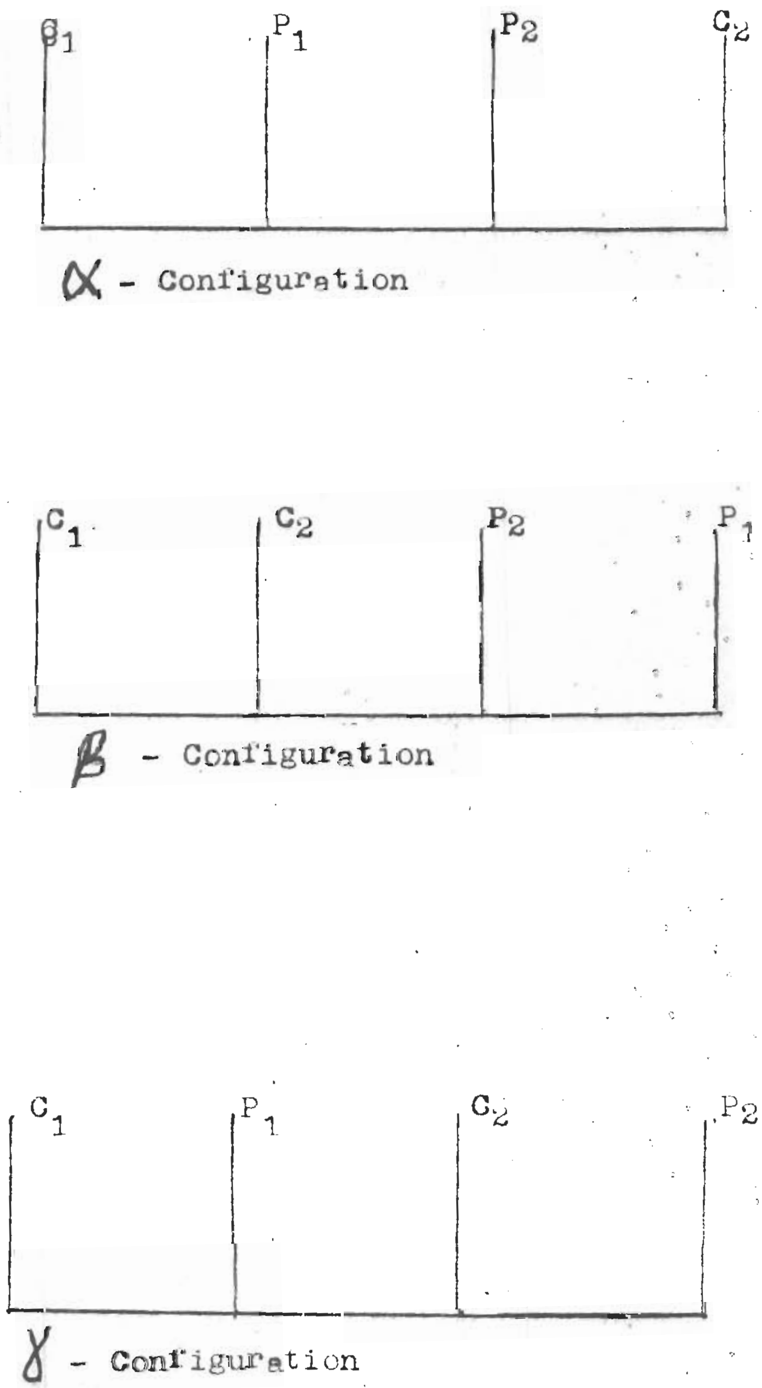

Figure 4 Principal tripotential configurations

In the Wenner tripotential system the electrode separations are the same. Using equation 4 in section 2.1, the apparent resistivities are derived as follows:

$$(1) \quad = \quad 2\pi \frac{\Delta V}{I} \quad \frac{1}{\left(\frac{1}{a} - \frac{1}{2a} - \frac{1}{2a} + \frac{1}{a}\right)}$$

$$= \quad 2\pi a \frac{\Delta V}{I}$$

$$\frac{\Delta V}{I} = \text{Resistance (R)}$$

$$\therefore \quad = \quad 2\pi aR \quad \ldots\ldots\ldots\ldots\ldots\ldots\ldots\ldots \quad (1)$$

a = Constant electrode separation.

(2) $$\rho^{\beta} = 2\pi R \left(\frac{1}{\frac{1}{3a} - \frac{1}{2a} - \frac{1}{2a} + \frac{1}{a}} \right)$$

$$= 2\pi R \left(\frac{1}{\frac{2}{6a}} \right)$$

$$= 2\pi R \, \frac{6a}{2}$$

$$\therefore \rho^{\beta} = 6\pi aR \quad \ldots\ldots\ldots\ldots\ldots\ldots\ldots \quad (2)$$

(3) $$\rho^{\gamma} = 2\pi R \left(\frac{1}{\frac{1}{a} \quad \frac{1}{a} \quad \frac{1}{3a} \quad \frac{1}{a}} \right)$$

$$= 2\pi R \left(\frac{1}{\frac{2}{3a}} \right)$$

$$= 2\pi R \, \frac{3a}{2}$$

$$\therefore \rho^{\gamma} = 3\pi aR \quad \ldots\ldots\ldots\ldots\ldots\ldots\ldots \quad (3)$$

Thus the apparent resistivities for the 3 electrode configurations are:

$$\rho^{\alpha} = 2\pi aR^{\alpha}$$
$$\rho^{\beta} = 6\pi aR^{\beta}$$
$$\rho^{\gamma} = 3\pi aR^{\gamma}$$

a = electrode separation

R^{α}, R^{β}, R^{γ} = measured α, β, γ resistances.

Carpenter (1955) studied the three resistances (R^{α} , R^{β} , R^{γ}) and has derived the following relation:

$$R^{\alpha} = R^{\beta} + R^{\gamma}$$

Substituting the values of the apparent resistivities in the above relation, he obtained another relation,

$$3\rho^{\alpha} = \rho^{\beta} + 2\rho^{\gamma}$$

It is therefore seem that if ρ^{γ} differs from ρ^{α} by an amount Y then ρ^{β} will differ from ρ^{α} by an amount -2y. The above relations are called the tripotential conditions.. This is obviously true in the case of homogenous and isotropic earth bounded by plane surface. Carpenter (1955) found out that any deviation from these conditions in resistances measured in the field and in the calculated resistivities indicates:

(1) Instrumental or observational error

(2) Lateral inhomogeniety like the presence of a sink.

The tripotential technique therefore provides a valuable a rapid means of identifying lateral variations in subsurface features from the measured resistances without having to convert them to their corresponding resistivities. These are the peculiar advantages of the technique. The extra labour involved in measuring three resistances rather than the conventional single resistance is very small, since once the cables have been laid out, all the terminal changes can be made at the instrument itself.

The tripotential technique has been applied successfully to some field problems. Carpenter (1955) applied this technique to longitudinal traversing perpendicular to the strike of a thin vertical insulating sheet and to another traversing across the strike of a simple vertical fault. The three apparent resistivities were plotted at the midpoints of measurements. He studied the behaviour of the three plots and found that when the electrode lines cross a lateral resistivity discontinuity, the apparent resistivities ρ^{α} and ρ^{γ} often as ρ^{β} decreases and vice versa. The effect of lateral resistivity variation will be clearly shown. If only the conventional curve is used, the effect of lateral resistivity variation would be much less obvious, and may lead to erroneous interpretation. Therefore plotting the three apparent resistivities leads to a better delineation of anomalous zones.

Another approach to the tripotential techniques was introduced by Kirk (1977) who also applied the method to the detection of fracture zones. This also involved running lateral traverses across the study area and taking the three resistance readings in every station. Kirk introduced what he called "Percentage residual resistivity" defined as:

$$(\rho^{\alpha} - \rho^{\beta} - \rho^{\gamma}) \times \frac{100}{\rho^{\alpha}}$$

The value obtained is plotted against horizontal distance in survey profile. The behaviour of the curve is studied and fracture zones can be located by the their resistivity anomalies. The anomaly interpretation can be done by resistivity modelling of fracture zones. Kirk also pointed out that the percentage residual resistivity method proved most useful in detecting the location, surface width and approximate depth of fracture zones. The method is particularly good in shale-sandstone terrain.

A variant of the technique for detecting cavities by the tripotential method was described by Habberjam (1969). This involved carrying out tripotential traverses over an area suspected to contain subsurface cavities. In this approach only the α and γ resistivity values are important. The ρ^{α} and ρ^{γ} values are plotted against midpoints of measurements along the traverses. From the α and γ curves, anomalous zones attributed....

to the presence of subsurface cavities can be delineated. These anomalies produced on the two curves can further be used to estimate the width and depth of burial of the cavities. According to Habberjam (1969), this is done by using two parameters, derivable from the curves, and which vary with h/r and a/r. "h" is the depth of burial of the cavities. "r" is the radius of the cavities (the cavities are regarded as spheres). "a" is the electrode spacing. The two parameters are called the "α-maximum" and "γ-fraction."

The "α-maximum" is the ratio of the central maximum value of α- resistivity to the value of the α-resistivity at a theoretically infinite distance from the sphere. Mathematically, this is expressed as

$$\frac{\rho^{\alpha}_{max}}{\rho^{\alpha}(\text{infinity})}$$

The central maximum value of α-resistivity is the α-resistivity value over the centre of the cavity or sphere. The resistivity at theoretically infinite distance from the sphere (cavity) is the α-resistivity least influenced by the sphere or the α-resistivity of the medium without the sphere (cavity).

The " γ -fraction" is the ratio of the mean value of the γ -resistivity at a distance from the surface centre of the sphere (cavity) equal to the electrode separation a, to the value of the γ - resistivity at an infinite distance from the sphere. The surface centre of the sphere is a point on the surface directly above the centre of sphere. Mathematically this parameter is expressed as:

$$\frac{\rho^{\gamma}_{a}}{\rho^{\gamma}\,(\text{infinity})}$$

The sphere in these definitions refers to the cavity. The γ -resistivity at theoretically infinite distance from the sphere is simply the γ -resistivity value of the medium without the sphere (cavity).

It is obvious from these definitions that the α -maximum and γ -fraction can be calculated from the anomalies produced by the cavities (regarded as spheres in the definitions above) on the α and γ curves respectively. Values of these parameters for values of a/r ranging from 0.5 to 5 and values of h/r ranging from 0 to 2 were obtained from tank experiments" conducted by Habberjam (1969) and the results were used to construct the curves of equal α -maximum values and equal γ -fraction values. This is shown in fugure 5. Within the observed ranges, each member of α-family of curves cuts any member of the γ-family of curves only once. Thus, from any specific value of the α-maximum and γ-fraction, a single intersection is obtained from which the a/r and h/r values are found. Since "a" would be known, r and h can be calculated.

The tripotential technique has proved very useful in detecting subsurface cavities. In this work the percentage residual resistivity method and Habberjam's approach in the interpretation have been adopted.

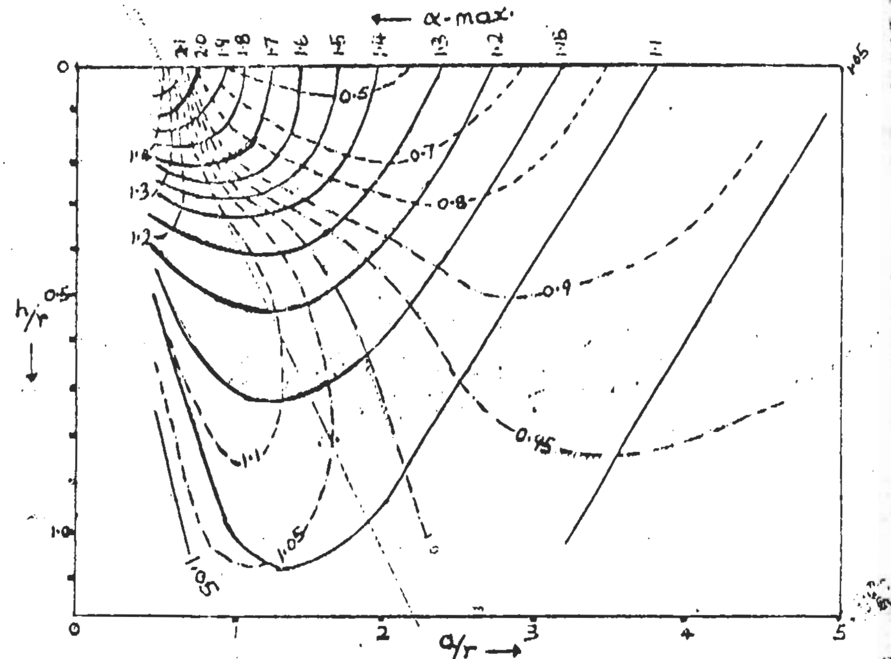

Figure 5 Family of curves of equal α - maximum and γ - fraction for interpretation of α and γ Configuration Wenner Resistivity data over a buried sphere.(Dashed lines represent α - curves while solid curves Show γ curves) Habberjam (1969)

2.3. INSTRUMENTATION AND FIELD PROCEDURES

2.3.1: Instrumentation

The equipment used in the work was the Abem Terrameter. It consists of a G-box and a V-box. The G-box contains the current supply unit consisting of a transistorised oscillator with batteries and operating controls. The V-box contains the potentional measuring units and the reference potentiometer circuit. The layouts of the G-box and V-box controls are shown in figure 6.

Operation of the Terrameter

From the V-box, the coarse gain control was set to position 0.1, thus switching the amplifier on, and a momentary deflection on the meter was observed. The output voltage selector in G-box was then set to 1/2 and current flow was indicated. This depended on the total resistance in the outer circuit. The selector could be set to 1/1 or a higher voltage when needed. By switching XR control to position X, amplifier was connected to potential electrodes, and the meter indicated a relative value of voltage Vx. In order to obtain a three-guarters fall scale deflection on the meter, the fine and coarse gain controls were adjusted; and by setting XR switch to position R, the relative value of voltage Vx was measured.

The reference potentiometer and potentiometer range control were continually adjusted until the meter deflection was observed. When meter reading was too low, the potentiometer knob was turned clockwise to increase R-reading, conversely, the digital potential was turned counter-clockwise to decrease R-reading.

Gain control was set in the same position as the potentiometer to obtain the same reading for position X and R. When gain control was reset, both X and R positions were checked again.

The readings were observed on the potentiometer scale and potentiometer range setting. 10 - turn scale read from 0 to 1000, number in scale window indicating hundreds. This was multiplied by factor indicated on the range knob.

After measurements, the amplifier was switched off by setting the gain control switch to position "OFF".

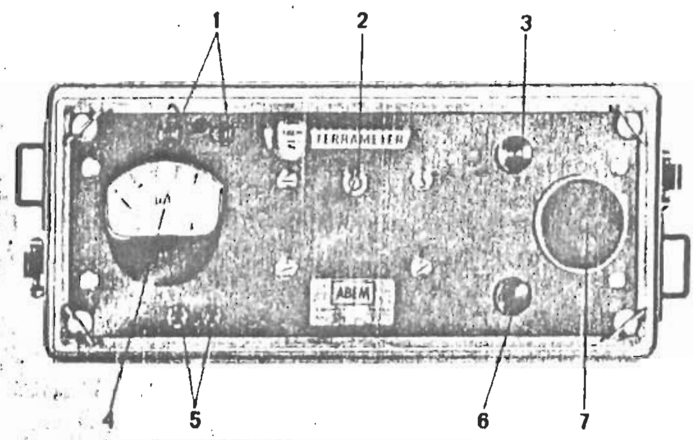

G-box controls

1. Current binding posts
2. Battery indicator
3. Output power selector
4. Output current indicator
5. Reference binding posts
6. Output voltage selector
7. Desiccator

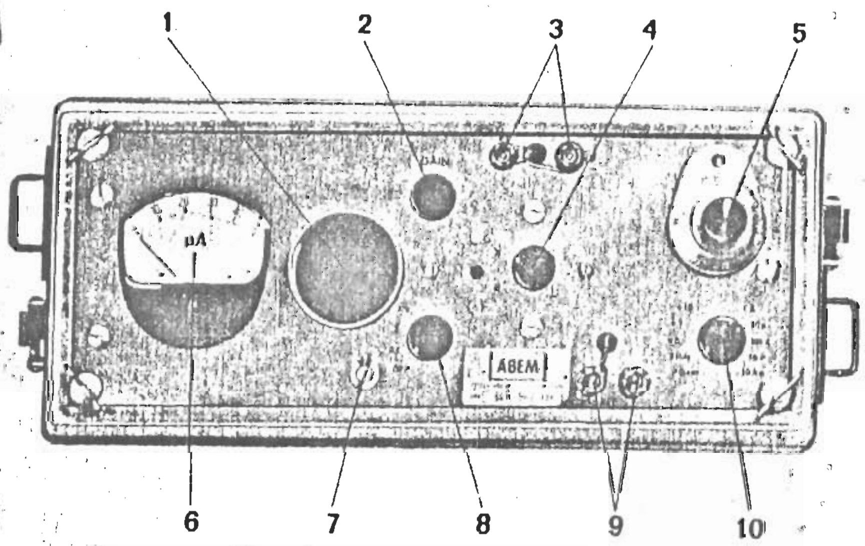

V-box controls

1. Desiccator
2. Fine gain control
3. Potential electrodes
4. X-R switch
5. Potentiometer control
6. Potential difference indicator
7. Battery indicator
8. Coarse gain selector
9. Reference binding posts
10. Potentiometer range

FIG. 6 THE G-AND V-BOXES OF THE ABEM TERAMMETER.

2.3.2: Field Procedures

Preliminary survey and archaeological data showed that the cavities were mostly concerntrated within the overburden with a maximum depth of 3m from the surface. Depth probing was also carried out earlier to determine vertical resistivity variation within the area.

The above information assisted in the selection of an electode spacing of 3m for the survey.

Thus the length of a typical array was 9m. The inter-electrode spacing of 3m was deemed suitable for exploring subsurface depths to the tune of 3m. The problem was to know whether this spacing was suitable for the sizes of the cavities. McCann et al (1987) have remarked that cavities whose widths were less than the electrode spacing cannot be detected. Some of the cavities already exposed by the excavation within the study area have sizes smaller than 3m. This posed a problem because smaller electrode spacing could not have been used for the survey as this would have become unsuitable for the depth of interest which was 3m. However, it was believed that part of the observed cavities may have been covered by later deposits. Therefore, the sizes of the cavities may be bigger than observed, probably as big as 3m. Furthermore, it was speculated that the cavities may be 3m or more since they were burial holes. It was on these assumptions that a spacing of 3m was selected as ideal for the survey.

The profiling was conducted along traverses at a bearing of 240^{o}E (see Figure 7). The interval between the traverses varied. The Western portion of the survey area had traverses located at distances ranging from 2 to 3m. This was particularly the area of interest where most of the cavities were thought to be concentrated. Larger intervals were used in the eastern portion.

Profiling along a traverse began at the northern end of the traverse, exactly from the Ogbodu Aba - Akpoga road. The

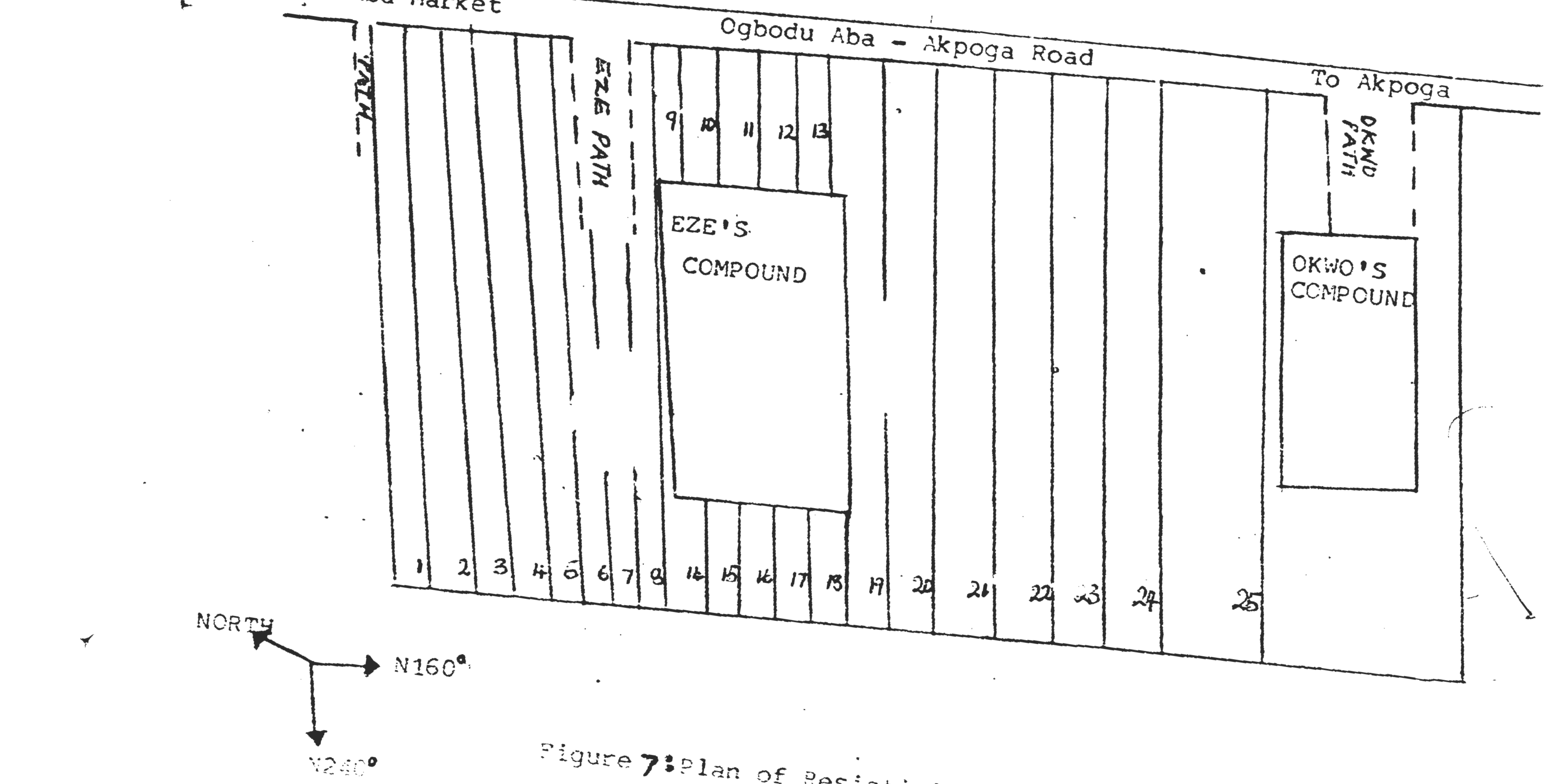

Figure 7: Plan of Resistivity Profiling in the study Area.

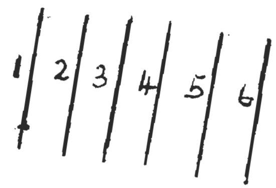

Traverse lines

traverses vary in length, ranging from 45m to those as short as 9m. The shorter traverses were run around Eze's compound (see fig. 7).

The interval between the measured positions along a traverse was 3m. At each position, 3 resistance values were obtained corresponding to the three different electrode arrangements described in section 2.2.2. This involved interchange of the electrodes to obtain the desired arrangement.

After the last reading R $(C_1P_1C_2P_2)$ has been obtained for each position, the electrodes were brought back to the first arrangement $(C_1P_1P_2C_2)$. Each electrode was then shifted 3m along the traverse direction. The new location of the electrode array constitutes the new measuring position and here, the whole procedure was repeated. This continued till the end of the traverse. The eletrodes were then transferred to the beginning of the next traverse and the procedure continued.

It is important to note that at each measuring position, the electrode array covered a distance of 9m along the traverse. The electrodes were also shifted 3m in order to place them to the next position. Thus starting from the beginning of a traverse, the distances covered by the electrode array for the successive measuring positions would be:

1 - 9m (1st position)

3 - 12 (2nd position)

6 - 15 (3rd position) etc.

2.4 Precautions taken in the field

1. The electrodes were driven deep into the ground to ensure good electrical contact with the ground.
2. The survey was conducted during the rainy season. This ensured enough ground moisture and thus enhanced electrical conductivity of the ground.
3. In areas where the ground was relatively dry and hard, salty water was added to the ground around the electrode positions. This also ensured good electrical contact with the ground.
4. The V-box and G-box were kept at a minimum separation of 50cm with their short sides facing each other.
5. The cables were not allowed to touch or run parallel for a very long distance.
6. The reels of the potential cables were oriented in such a way that they were made perpendicular to the current cables.

N/B. Precautions 4,5,6 were also done to avoid induction effects.

7. The wires tied to the electrodes were regularly examined to make sure they were in-tight. The cables were also regularly checked to ensure that no naked wire was exposed along them.

8. Large stones and other conducting materials around the position of the electrodes were removed. This prevents irregular influences on the reading.

2.5 Presentation of Data

A total of 25 traverses were run within the entire area and 175 readings were obtained. The resistance values were converted to their apparent resistivities using the formulae given in section 2.2.2.

The expressions for the apparent resistivities of the 3 resistances were given as:

$$\rho^{\alpha} = 2\pi aR$$

$$\rho^{\beta} = 6\pi aR$$

$$\rho^{\gamma} = 3\pi aR$$

where ρ^{α}, ρ^{β} and ρ^{γ} are apparent resistivities for the electrode arrangements $C_1P_1P_2C_2$, $C_1C_2P_2P_1$ and $C_1P_1C_2P_2$ respectively while R^{α}, R^{β} and R^{γ} are their corresponding resistances.

The electrode spacing is denoted as a and this was 3m. Substituting this in the above formulae gives:

$$\rho^{\alpha} = 2 \times 3.14 \times 3 \times R = 18.84R$$
$$\rho^{\beta} = 6 \times 3.14 \times 3 \times R = 56.52R$$
$$\rho^{\gamma} = 3 \times 3.14 \times 3 \times R = 28.26R$$

Using the above derivations, the apparent resistivities for the 175 resistance values were computed. These are presented in table 2 of the Appendix. The apparent resistivities were also written against their locations on a map of the area and a contoured resistivity map of the study area was produced. This is shown in the attached map (fig. 16)

The percentage residual resistivities of the 175 calculated apparent resistivities were also computed. The computed percentage residual resistivities are presented in table 2.

CHAPTER THREE

INTERPRETATION

The interpretation procedures adopted here were both qualitative and quantitative. The major aim was to identify any anomalous zones within the area and to analyse them and estimate the dimensions and depths of burial of any cavities that may be present.

3.1 Plotting of Resistivity Values

For every traverse, three types of plots have been made using the apparent resistivity values obtained along the traverse. The three types of plots are:

(1) The α-plot

(2) The γ-plot

(3) The percentage residual resistivity plot.

The α-plot is a plot of the calculated α-apparent resistivity values for any traverse against the midpoints of measurements along the traverse.

The γ-plot is also a plot of the γ- apparent resistivities for any traverse against the midpoints of measurements along the traverse.

The percentage residual resistivity plot is also a similar plot but using the computed percentage residual resistivity values along any traverse.

It is important to note that no β-plots have been made. This was because the above three types of plots were the only plots necessary and sufficient for the method of interpretation adopted here. The α and γ plots sufficiently defined the anomalous zones along any traverse. Furthermore, they were the only plots used in the calculation of the dimensions of the identified cavities given in chapter 4.

The three types of plots have been made for traverses 1, 2, 3, 4, 5, 8, 19, 20, 21, 22, 23, 24. Few readings were obtained along traverses 6 and 7 thus no plots have been made for these traverses. Traverses 9 to 13 and 14 to 18 were two sets of short traverses infront and behind Eze's compound respectively (See Figure 7). Only one reading was obtained in each of these traverses. Thus , and percentage residual resistivity plots for each of these traverses were not possible. Alternatively, a profile cutting across traverses 9 to 13 and cutting 14 to 18 have been taken. These are called profiles 9 and 10 respectively. Each profile was taken in such a way that it passed through the midpoints of the electrode spreads of the measurements in each traverse (i.e. at 4.5m along each traverse.).

α, γ and percentage residual resistivity plots were then made for the two profiles.

It is also important to note that no measurements were made between 18 and 27m along traverse 19. This was the location of a toilet pit. This gap was reflected in the plots. Figures 8 to 15 show all the plots.

3.2 Description of the profiles and delineation of Anomalous zones

The behaviour of the α, γ and percentage residual resistivity curves for any traverse were studied and compared. Anomalies were then delineated taking into consideration the following points.

1. The actual behaviour of the curves thus noting any points that showed a significant deviation from the general trend.
2. The Overall agreement of the α, γ and percentage residual resistivity curves for any traverse.
3. The fulfilment of the tripotential condition by the resistance values used in calculating the apparent resistivities that were plotted around the deviating point. The non-fulfilment of this condition is an indication of lateral inhomogeniety within the ground.

Based on these considerations 6 traverses were considered significant because of the anomalies picked along them. These were traverses 5, 8, 19, 21 and profiles 9 and 10.

The remaining traverses showed no anomalies. The resistivity values obtained along them renged between 300 and 600 Ω m. This corresponded to that of loamy soil which was in fact the dominant lithology of the study area. In many of the traverses, the α and γ plots showed good agreements. Some tended to be flat while others showed undulating behaviour. This undulating behaviour was attributed to the effect of irregularities on the readings.

Traverse 5 (Figures 10a, b)

The α and γ curves showed a good match. An anomaly occurred on both curves between 4.5m and 10m. This was a high resistivity anomaly as both curves rose above the general trend between these distances. In the case of the percentage residual resistivity curve, the anomaly occurred at the edge of the curve at 4.5m. Here, it showed a lower value then the general trend. The Resistance values obtained within this anomalous zone also did not obey the tripotential condition ($R^{\alpha} = R^{\beta} + R^{\gamma}$). ($R^{\alpha} - (R^{\beta} - R^{\gamma})$) values for the two measured stations within the zone (1-9m and 3-12m) are 7.20 and 4.23. These are anomalous since they deviated very well from zero. Based on this comparison, the anomaly occurring on this traverse was delineated between 4.5m and 10m. The centre and peak of the anomaly occurred at 7.5m along the traverse.

Traverse 8 (Figures 10a, b)

The traverse covered a distance of 45m. The percentage residual resistivity curve showed a complex behaviour.

The resistance values between distances 6 to 45m were also confusing. All the values did not obey the tripotential condition, apparently indicating many anomalies. The seemingly numerous anomalies were however compared with those on the α and γ curves and a better delineation was made. On the overall, two prominent anomalies were picked. These occurred between 13.5 and 19.5m and between 31.5 and 40.5m. Their centres and peaks occurred at 16.6m and 37.5m respectively.

Profile 9 (Figures 11a, b)

This was the profile that cut across traverse 9 to 13. It covered a distance of 14m. The three curves showed a high anomaly at 5m along the profile. Another high anomaly was shown by the α and γ curves at 11m. This anomaly was also shown as a low anomaly on the percentage residual resistivity curve at 11m. The $\left(R^{\alpha}-(R^{\beta}-R^{\gamma})\right)$ Values of 5 and 3.4 obtained around the two anomalies were also anomalous since they deviated significantly from zero.

Profile 10 (Fig. 11a, a)

This was the profile that cut across traverses 14 to 18. It also covered a distance of 14m. The α, γ and percentage residual resistivity curves showed a high anomaly between 5 and 8m. The centre and peak value of this anomaly was taken to be at 6.3m along the profile. This anomaly correlated very well with the anomalous value of $(R^{\alpha} - (R^{\beta} - R^{\gamma}))$ obtained within the zone. The value was 3.85.

Traverse 19 (Figures 12a, b)

A distance of 45m was covered by this traverse. The three curves showed a prominent high resistivity anomaly with centre and peak value at 10.5m. The tripoteatial condition was also not fulfilled within this zone (distance 6-15m). $(R^{\alpha} - (R^{\beta} - R^{\gamma}))$ value obtained was 3.00. The α and γ curves remained flat along the rest of the traverse. However, the percentage residual resistivity curve showed a very low value at the right edge of the curve. The possibility of an anomaly was ruled out when this was compared with the α and γ curves.

Traverse 21 (Figures 13a, b)

The traverse also covered a distance of 45m. The three curves showed high values at the left edge of the traverse. Details of this anomaly could not be known since it occurred at the edge. It was therefore not considered significant. Another anomaly was observed on the three curves at 22.5m. The α and γ curves showed this as a high anomaly while the percentage residual resistivity curve showed this as a low anomaly.

This anomaly correlated very well with the anomalous (R - (R - R)) value of 9.58 obtained within zone (distance 18-27m).

From the above discription, eight anomalous zones have been delineated. These are summarized in table 3 below. This is in line with the observations of McCann et all (1987) who earlier found that air-filled cavities have higher resistivities than the host rock, but that the same cavities would have lower resistivities if they were filled with conductive materials.

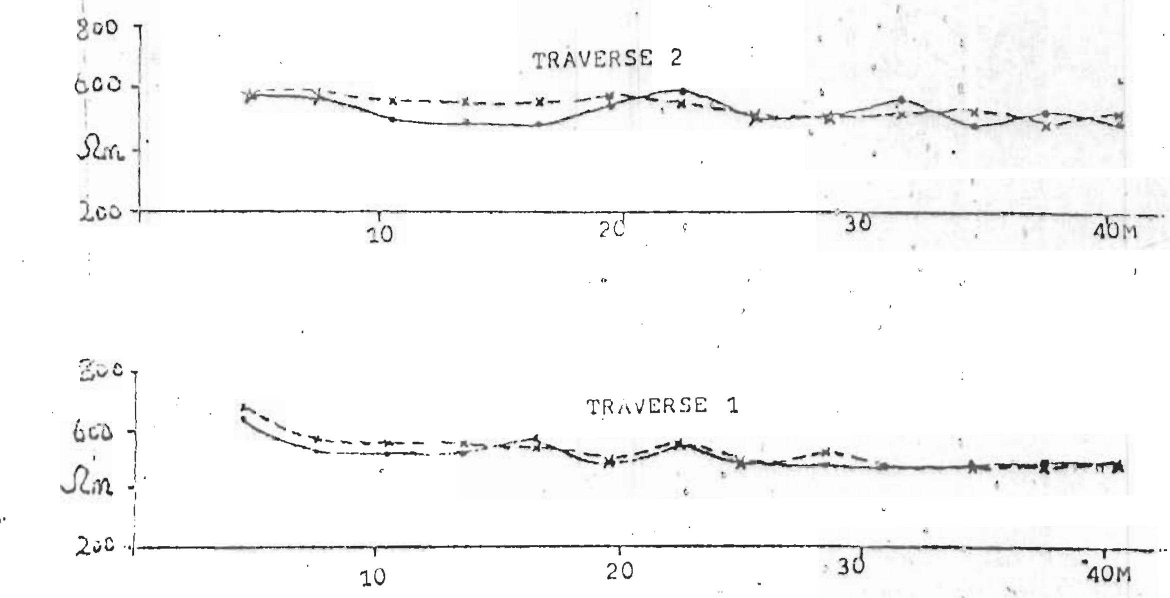

Figure 8a: α and γ plots for traverses 1 and 2.

(Solid curves show α plot while dotted curves indicate γ plots)

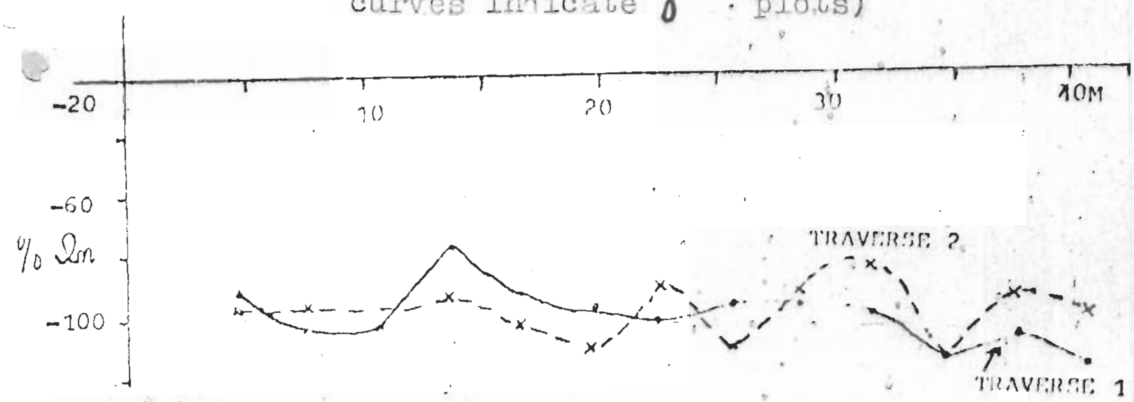

Figure 8b: Percentage Residual Resistivity plots for traverses 1 and 2

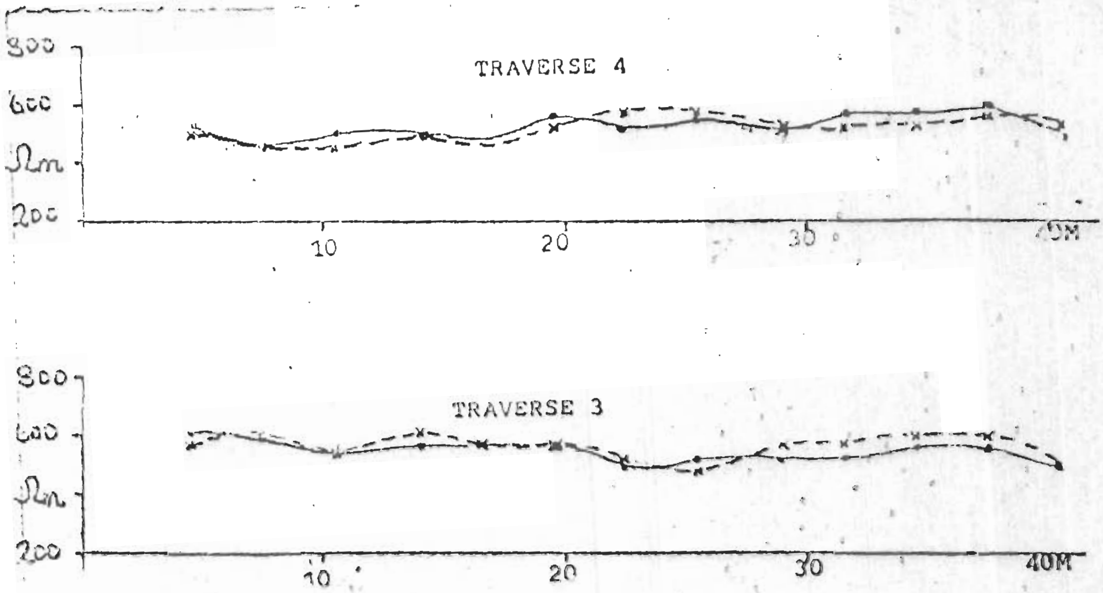

Figure 9a: α and γ plots for traverses 2 and 3.

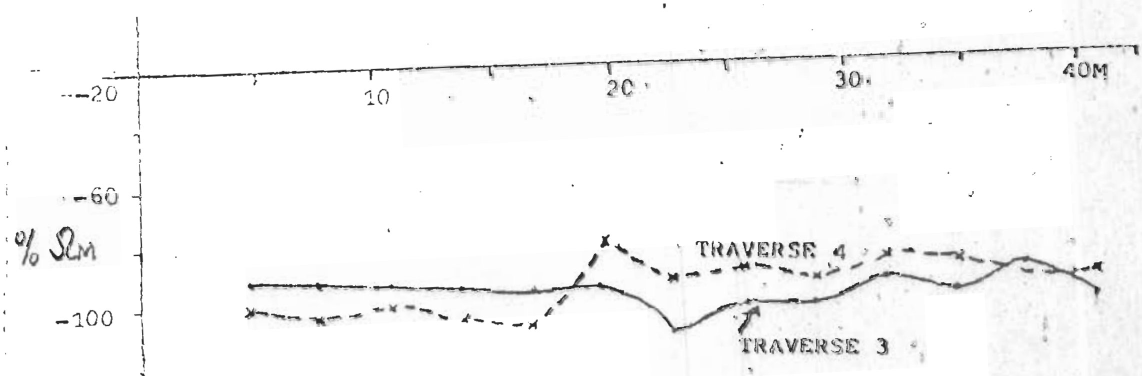

Figure 9b. Percentage Residual Resistivity plots for traverses 3 and 4

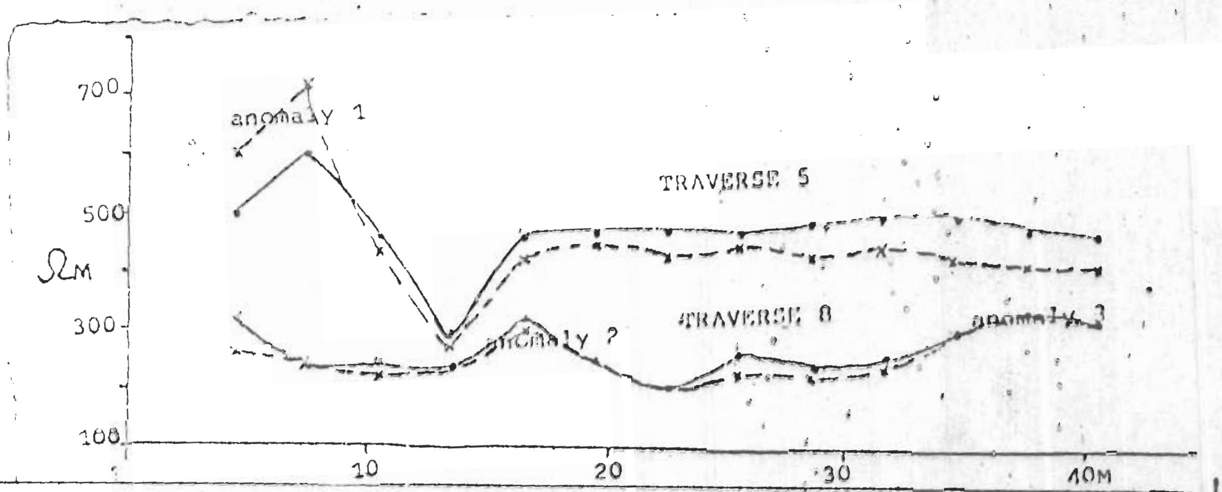

Figure 10a: α and γ plots for traverses 5 and 8.

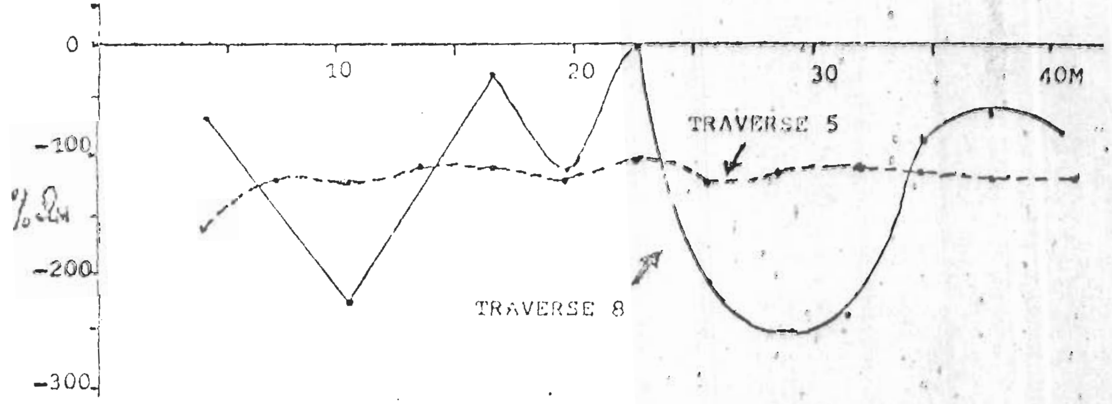

Figure 10b: Percentage Residual Resistivity plots for traverses 5 and 8

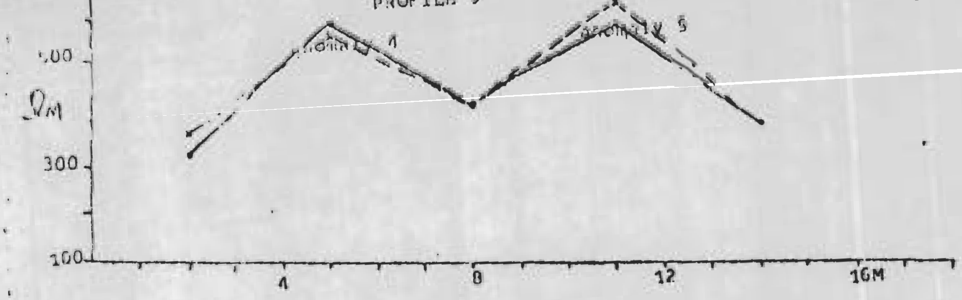

Figure ||a: α and γ plot for profiles 9 and 10

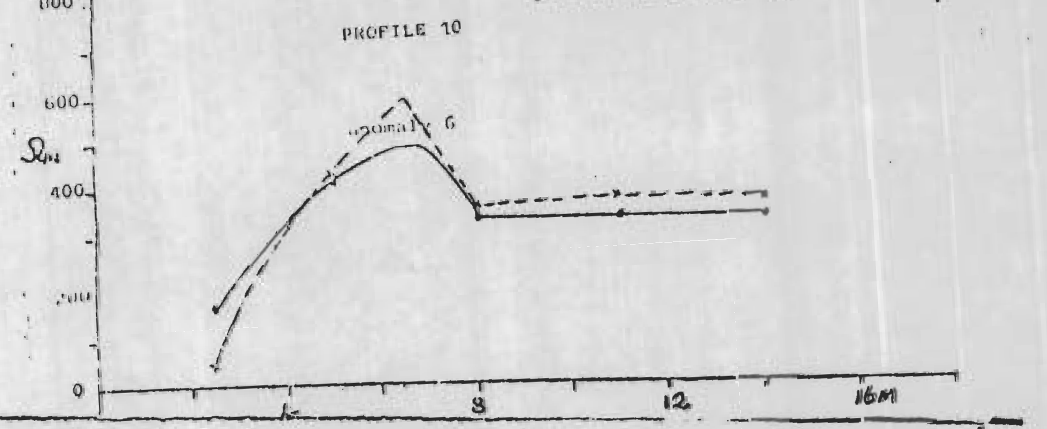

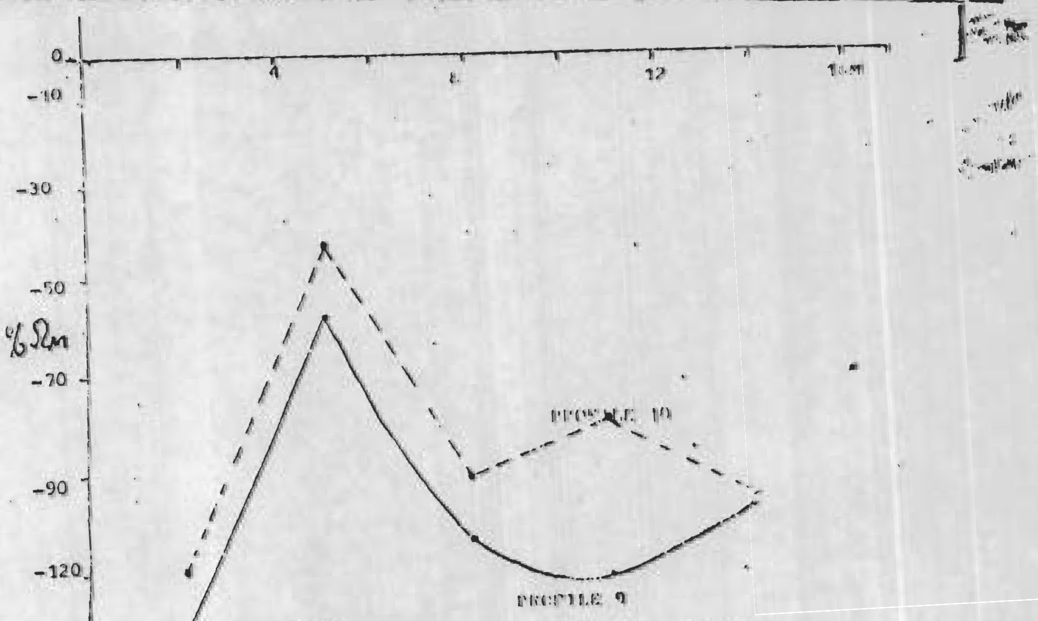

Figure ||b: Percentage residual resistivity plots for profiles 9 and 10

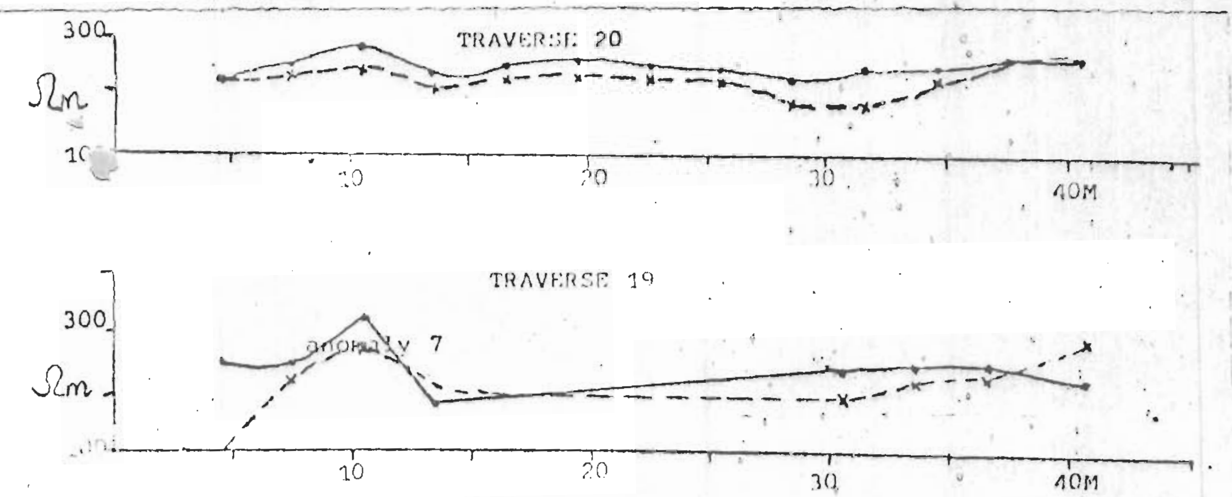

Figure 12a: α and γ plots for traverses 19 and 20

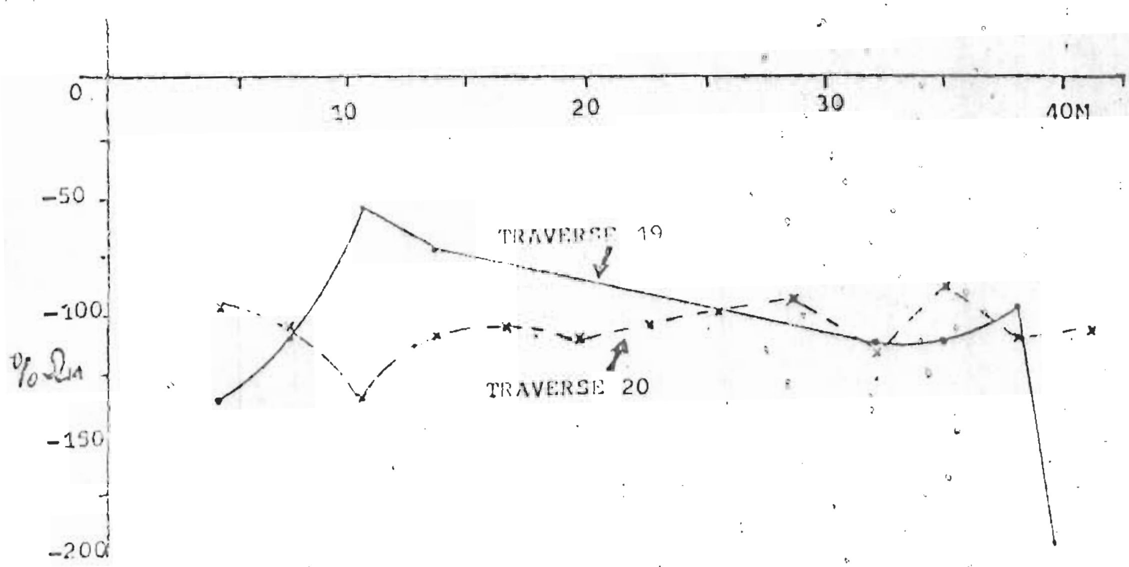

Figure 12b: percentage risdual resistivity plots for traverses 19 and 20.

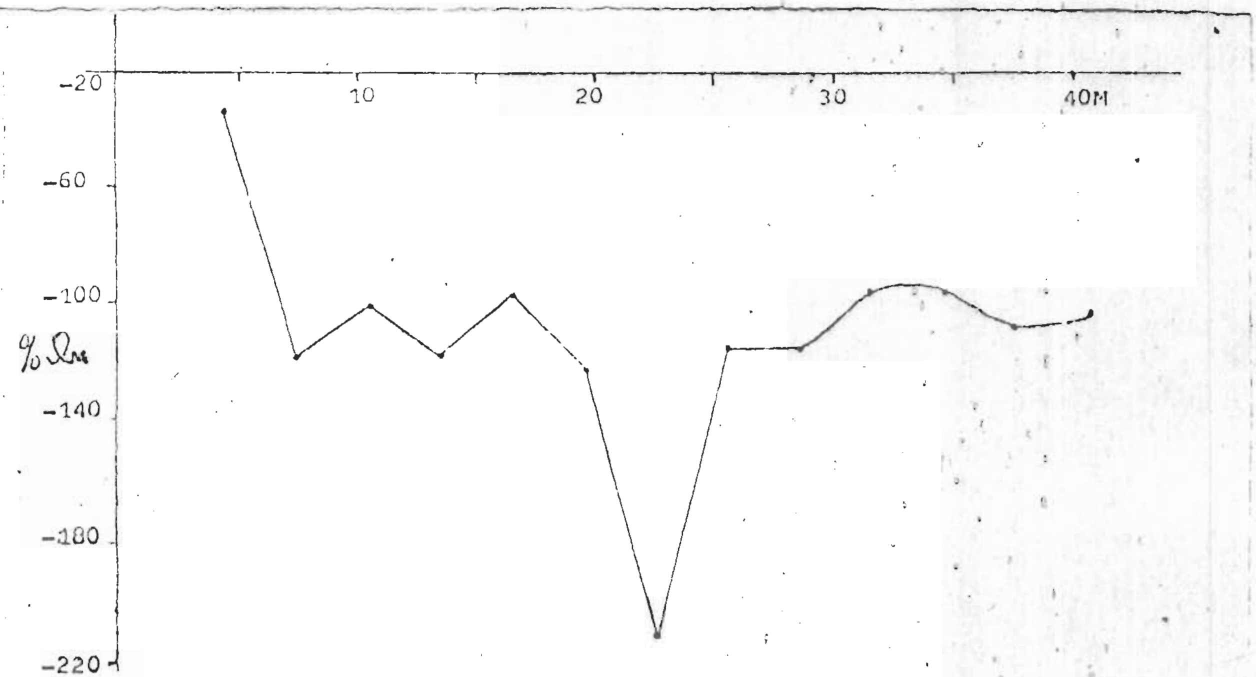

Figure 13a: Percentage residual resistivity plots For traverse 21.

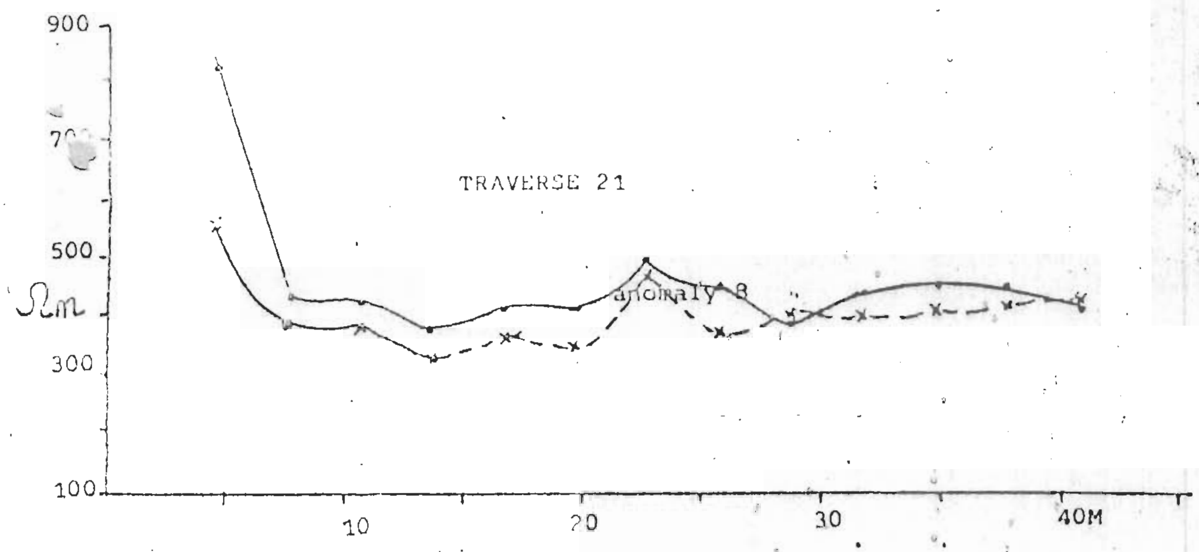

Figure 13b: α and γ plots for traverses 21

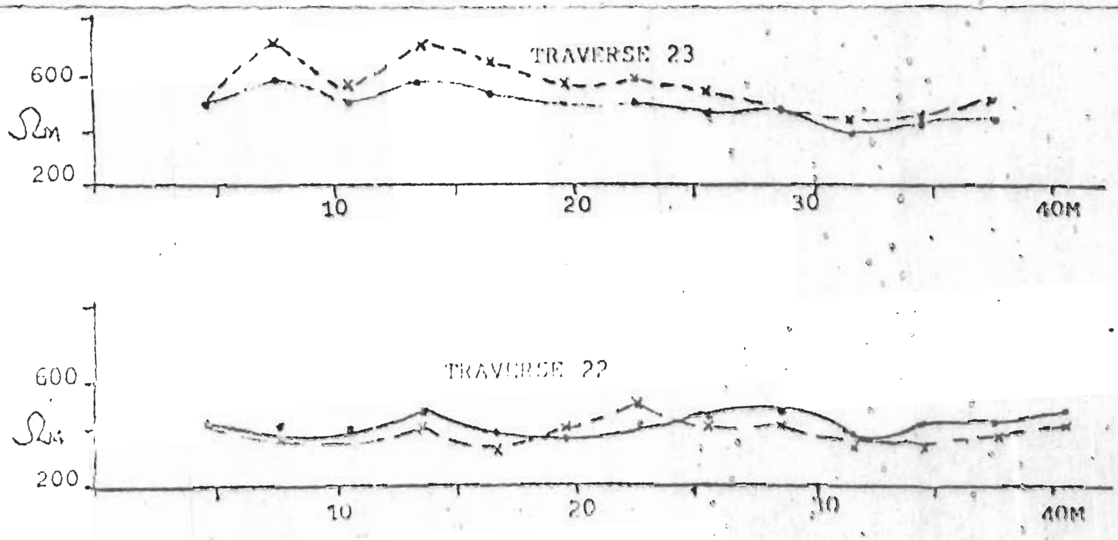

Figure 14a: α and γ Plots for Traverses 22 and 23

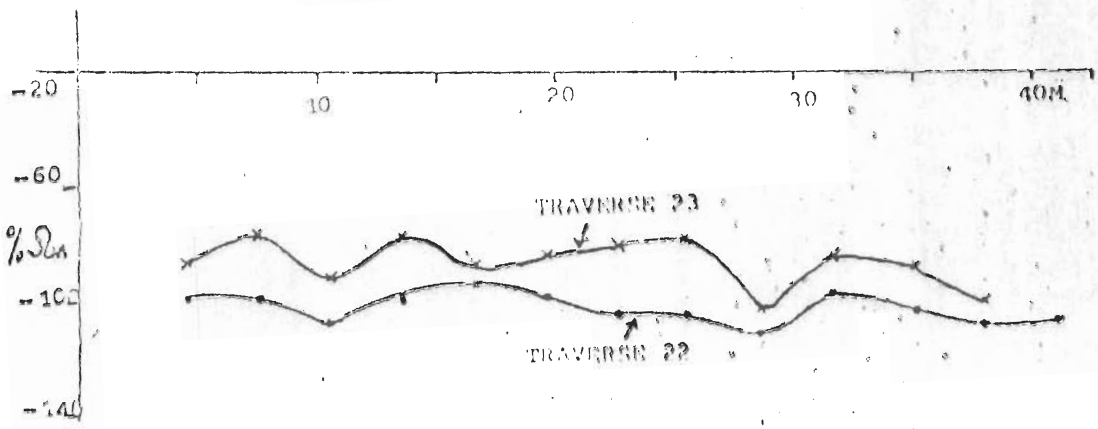

Figure 14b: Percentage Residual Resistivity Plots for Traverses 22 and 23

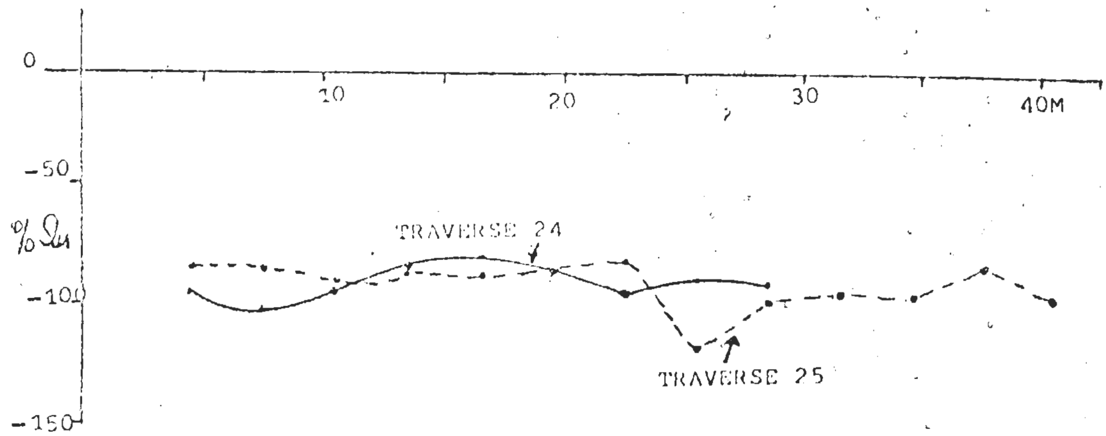

Figure 15a: percentage Residual Resistivity plots for Traverses 24 and 25

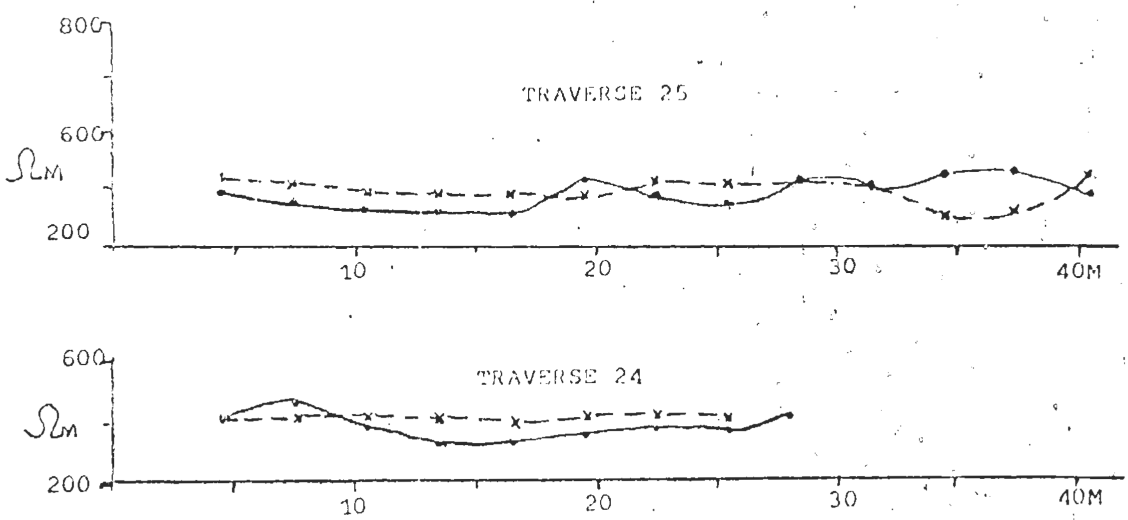

Figure 15b: α and γ plots for Traverses 24 and 25

Table 3: Delineated Anomalous Zones

S/No.	Traverse	Centre and location of peak of anomaly along the traverse
1.	5	7.5m
2.	8	16.5m
3.	8	37.5m
4.	Profile 9 (traverse 9 to 13)	5m
5.	Profile 9 (traverse 9 to 13)	11m
6.	Profile 10 (traverse 14 to 18)	6.3m
7.	19	10.5m
8.	21	22.5m

CHAPTER FOUR

4.1 Discussion of the Results

The major zone of the subsurface investigated in this work was the overburden which has an average thickness of about 3m. Hydrogeological data from the area indicate that the water table occurs at much deeper levels (>10m). In the interpretation of the resistivity anomalies, one can rule out the influence of groundwater (including the possibility of water filled sink-holes) in the area. It appears reasonable in the light of archaeological information from the area to interprete the detected anomalous zones in terms of cavities located within the overburden. The cavities and their contents of human bones and iron tools are attributed to be the sources of the resistivity anomalies. Table 4 gives a summary of the dimensions of the interpreted cavities whose locations are indicated on the contoured map shown on Figure . The sizes and depths of burial of the cavities were estimated using Habberjam's technique described in chapter two. The centres of the anomalous zones were regarded as the centres of the cavities.

The resistivities of the cavities were all consistently much higher than those of the host rocks. The cavities can therefore be better interpreted as hollow or air-filled cavities.

Table 4: Sammary of the dimensions of possible cavities

S/NO	Traverse	Resistivity value over centre of the cavity (Ω m)	Radius cavity (m)	Depth of bu rial (m)
1.	5	600	2.00	0.80
2.	8	320	1.76	0.84
3.	8	400	6.00	1.50
4.	Profile 9	590	2.70	0.94
5.	Profile 9	590	2.10	0.67
6.	Profile 10	500	2.70	0.78
7.	19	310	2.00	0.70
8.	21	500	1.50	0.55

The above eight possible cavities identifed have been based on the anomalies observed on the curves. Two, out of thise eight were known cavities. These are cavities nos. 2 and 6. The resistivity value over cavity no 2 was not as high as those of other cavities. The relatively lower value may be caused by some infills.

In spite of errors that would be present in the interpretation, there is a high probability that several of the identified cavities may actually be present within the delineated areas. Cavity no. 1 for instance showed a high resistivity anomaly of 600Ω m that stood out prominently from the general trend in resistivities which averaged 450Ω m along the traverse. The estimated radius of 2m is consistent with those of the known cavities. Although the calculated depth of burial is small (0.8m), one may not rule out the influence of such factors like survace erosion in reducing the depth to the subsurface cavities. This is most probable considering that the cavities were located on top of a hill.

Cavity no. 3 showed exceptionally large radius. There is a very little probability of having a cavity with this size within the study area. The actual presence of this cavity is therefore doubtful. Perhaps, this was the location of a discused pit, filled up with later deposits and thus appeared anomalous on the plots. Cavity numbers 4 and 5 showed high resistivity values (590Ω m) that stood out prominently above the general trend along their traverses. The sizes and depths were also consistent with those of the known cavities. Cavities nos. 7 and 8 showed resistivity values slightly above the general trend along their respective traverses. While this did not provide a strong evidence for the actual presence of these cavities, the relatively the low values, probably may have been caused by some infilling material.

On the whole, one would recommend that 3 out of the 8 possible cavities be exc_avated. The recommended drilling locations are cavities nos. 1, 4 and 5.

4.2 Conclusion and Recommendation

This work has identified eight anomalous locations thought to be possibly caused by the presence of buried cavities in the studied area. The anomalies were attributed to the presence of buried cavities based on available geological and archaeological information. Furthermore, the estimation of depths and sizes of these cavities have also been made on the assumption that these features are air-filled. Like other geophysical surveys of this type, the results presented here are subject to confirmation in the form of test-excavation in the delineated area. Logistic problems and non-availability of funds hindered the inclusion of this confirmatory test in this work.

However, cavities 1, 4 and 5 are strongly recommended for digging since they Showed the greatest possibility of actually being present in the area.

The location of these cavities were shown as shaded zones in the attached map (Figure 16). The locations and extent of the other cavities have also been shown on figure 16. Considering that errors may arise from theoretical estimations, it is therefore important to regard the estimated sizes of the cavities as approximate ranges of lengths within which the cavities may be found. Also the estimated depths may be looked on as minimum depths that can be dug before encountering the cavities if they are actually present. The maximum depth would be 3m since this was the maximum depth of investigation.

REFERENCES

Bristow, C. 1966. A new graphical resistivity method for detecting air-filled cavities. Studies in Speleology, Vol. 1, P. 204 - 227.

Carpenter, E.W., 1955. Some notes concerning the Wenner configuration. Geophysical prospecting, Vol. 3, p. 388 - 402.

Carpenter, E.W. and Habberjam G.M., 1956. A tripotential method of resistivity prospecting. Geophysics, vol. 21, P. 455 - 469.

Chikwendu. F., 1980. Ogbodu Aba Burial Chambers. Paper presented at the national symposium on African Arts and Culture. Institute of African Studies, U.N.N.

Dobrin, M.B., 1976. Introduction to Geophysical Prospecting. McGraw-Hill, Tokyo.

Greenfield, R.J., 1979. Review of geophysical approaches to the detection of Karst. Bulletin of the Association of Engineering Geologists. Vol. 16, P. 393 - 408.

Griffiths, D.H. and King, R.F., 1965. Applied Geophysics For Engineers and Geologists. Pergamon Press.

Habberjam, G.M., 1969. The location of spherical cavities using a tripotential resistivity technique. Geophysics Vol. 34, No. 5 P. 780 - 784.

Kirk., 1977. Location of Fracture Zones using Tripotential Resistivity methods. EOS Vol. 58, No. 6, P. 392.

Kook, K.L. and Nostrand, R.G.V., 1953. Interpretation of resistivity data over filled sinks. Geophysics. Vol. 19, P. 761 - 790.

Kunetz, G., 1966. Principles of direct current resistivity Prospecting. Geoexploration monographs series, No. 1 P. 103, Gerbruder Borntoiger Berlin.

Lancaster, J.E., 1930. The Earth resistivity method of Geophysical Prospecting. Mining Magazine, Vol. 42, P. 355 - 360 and Vol. 43, P. 19 - 68.

Love, C.L., 1966. Geophysical study of highway Problems in Limestone terrain .California Division of Highways Research Report No. M & R 64270, 50-62

Maxwell, G.M., 1976. Old Mine Shafts and their location by geophysical surveying. Quarterly Journal of Engineering Geology, Vol. 9, P. 283 - 290.

McCann, D.M., Jackson, P.D. and Culshaw, M.G., 1987. The use of geophysical surveying methods in the detection of natural cavities and mineshafts. The Quarterly Journal of Engineering Geology, Vol. 20, No. 1, P. 73.

McDowell, P., 1975. Detection of clay filled sinkholes in the chalk by geophysical methods. Quarterly Journal of Engineering Geology, Vol. 8, P. 303 - 310.

Owen, T.E. and Suhler, S.A., 1980. Subsurface void detection using surface resistivity and borehole electromagnetic techniques. Paper E-7, Society of Exploration Geophysics, Tilsa.

Palmer, L.S., 1954. Location of Subterranean cavities by geoelectrical methods. The Mining Magazine, Vol. 91, P. 131 - 141.

Parasnis, D.S., 1966. Mining Geophysical, Methuen London.

Roman, 1., 1931. How to compute Tables for Determining Electical Resistivity of underlying Beds and their application to Geophysical Problems. U. S. Tech. Pub. 502, P1-44

Sarma V.VJ., 1961. Modified Tripotential prospecting method. Geophysical prospecting, Vol. 11, P. 16 -18.

Sarma, V.V.J., 1963. A General Formula tripotential prospecting method. Geophusical prospecting, Vol. 11, P. 16-18.

Slitcher, L.B., 1933. The interpretation of the resistivity prospecting method for horizontal structures. Physics, Vol. 4, P. 307 - 322.

Spiegel. R.J., 1980. Modelling of resistivity anomalies from localized voids under irregular terrain. Geophysics, Vol. 45, No. 7, P. 1164.

Van Nostrand, R.G., 1953. Limitations on resistivity methods as inferred from the buried sphere problem. Geophysics, Vol. 18, P. 423 - 433.

Vingoe, P., 1972. Electrical resistivity Surveying, Geophysical memorandum 5/72, ABEM Printed Matter No. 90019.

Wynn, J.C., 1986. Archaeological prospection: An introduction to the special issue. Geophysics, Vol. 51, No. 3, P. 533 - 537.

TABLE 2: RESISTIVITY DATA

TRAVERSE	S/No.	DISTANCE MEASURED ALONG TRAVERSE	MID POINT OF MEASURED DISTANCE	R^{α}	R^{β}	R^{γ}	ρ^{α} (Ωm)	ρ^{β} (Ωm)	ρ^{γ} (Ωm)	PERCENTAGE RESIDUAL RESISTIVITY
1	1	1-9m	4.5	34.1	10	23.8	642	565	673	-92
	2	3-12	7.5	30.9	11	20.2	582	622	571	-104
	3	6-15	10.5	29.6	9.8	21.1	558	554	596	-106
	4	9-18	13.5	31.2	8.7	19.9	588	492	563	-79
	5	12-21	16.5	30.8	10	19.8	580	565	560	-93
	6	15-24	19.5	27	8.9	18.0	509	503	509	-98
	7	18-27	22.5	30	10.2	20	565	577	565	-102
	8	21-30	25.5	27.6	9	18.4	520	509	520	-97
	9	24-33	28.5	29	9.4	19.2	546	531	543	-96
	10	27-36	31.5	27	9.0	18.1	509	509	512	-100
	11	30-39	34.5	28	11.2	18	528	633	509	-116
	12	33-42	37.5	28	10.5	17.9	528	593	506	-108
	13	36-45	40.5	27	11	17.5	509	622	495	-119

TRAVERSE	S/No.	DISTANCE MEASURED ALONG TRAVERSE	MID POINT OF MEASURED DISTANCE	R^{α}	R^{β}	R^{γ}	ρ^{α} (Ωm)	ρ^{β} (Ωm)	ρ^{γ} (Ωm)	PERCENTAGE RESIDUAL RESISTIVITY
2	1	1-9	4.5	31	9.8	21.1	584	554	596	-97
	2	3-12	7.5	31.4	10.2	20.6	592	577	582	-96
	3	6-15	10.5	28.7	9.6	20	541	543	565	-105
	4	9-18	13.5	29.2	8.8	19.9	550	497	562	-93
	5	12-21	16.5	29.1	8.7	20	548	492	565	-93
	6	15-24	19.5	30	10.5	21	565	593	593	-110
	7	18-27	22.5	31.8	10.3	19.8	600	582	560	-90
	8	21-30	25.5	27.5	10	18.6	518	565	527	-111
	9	24-33	28.5	27.9	8.6	18.5	526	486	523	-92
	10	27-36	31.5	30.5	9.4	19	575	531	537	-86
	11	30-39	34.5	27	10	19.1	509	565	540	-117
	12	33-42	37.5	28.8	9.5	18.2	543	537	514	-94
	13	36-45	40.5	26.6	8.3	19.1	501	469	540	-101

..../53

TRAVERSE	S/No.	DISTANCE MEASURED ALONG TRAVERSE	MID POINT OF MEASURED DISTANCE	R^{α}	R^{β}	R^{γ}	ρ^{α} (Ωm)	ρ^{β} (Ωm)	ρ^{γ} (Ωm)	PERCENTAGE RESIDUAL RESISTIVITY
3	1	1-9m	4.5	32.6	10.4	21.1	614	588	596	-93
	2	3-12	7.5	32.3	10.1	21.6	609	571	610	-94
	3	6-15	10.5	29	9.2	19.3	546	520	545	-95
	4	9-18	13.5	31.2	9.7	21.7	588	548	613	-97
	5	12-21	16.5	31	9.8	21.2	584	554	599	-97
	6	15-24	19.5	31.7	10.5	20.6	597	594	582	-97
	7	18-27	22.5	27.4	10.1	18.9	516	571	534	-114
	8	21-30	25.5	28.5	10.6	17.7	537	599	500	-105
	9	24-33	28.5	28.5	9.4	20.2	537	531	571	-105
	10	27-36	31.5	29.5	9.1	20.2	556	514	571	-95
	11	30-39	34.5	31.6	10.1	22.2	595	571	627	-101
	12	33-42	37.5	30.7	8.8	21.5	578	497	608	-91
	13	36-45	40.5	27.5	9.7	18.2	518	548	514	-105

TRAVERSE	S/No.	DISTANCE MEASURED ALONG TRAVERSE	MID POINT OF MEASURED DISTANCE	R^{α}	R^{β}	R^{γ}	ρ^{α} (Ωm)	ρ^{β} (Ωm)	ρ^{γ} (Ωm)	PERCENTAGE RESIDUAL RESISTIVITY
4	1	1-9	4.5	28	9.6	18.5	528	543	523	-102
	2	3-12	7.5	25	9	16.3	471	509	461	-106
	3	6-15	10.5	27	10.1	16.1	509	571	455	-102
	4	9-18	13.5	27	9.6	18.3	509	543	517	-108
	5	12-21	16.5	25	9	17	471	509	480	-110
	6	15-24	19.5	30	9.2	18.9	565	520	534	-81
	7	18-27	22.5	27.6	7.5	20.6	520	424	582	-94
	8	21-30	25.5	30	8.9	20.4	565	503	577	-91
	9	24-33	28.5	28	8.8	19	528	497	537	-96
	10	27-36	31.5	31	10	18.9	584	565	534	-88
	11	30-39	34.5	31	10.2	18.9	584	577	534	-90
	12	33-42	37.5	32	11	20.5	603	622	579	-99
	13	36-45	40.5	26	7.5	19	490	424	537	-96

TRAVERSE	S/No.	DISTANCE MEASURED ALONG TRAVERSE	MID POINT OF MEASURED DISTANCE	R^{α}	R^{β}	R^{γ}	ρ^{α}	ρ^{β}	ρ^{γ}	PERCENTAGE RESIDUAL RESISTIVITY
5	1	1-9m	4.5	26.53	12.5	21.23	500	707	600	-161
	2	3-12	7.5	31.84	10.6	25.47	600	599	720	-119
	3	6-15	10.5	24.6	10.8	15.6	463	610	440	-126
	4	9-18	13.5	14.2	4.5	10.5	267	254	297	-106
	5	12-21	16.5	24.6	11.4	14.9	463	644	421	-130
	6	15-24	19.5	25.1	10.2	15.9	473	576	449	-117
	7	18-27	22.5	25.3	9.6	15.4	477	543	435	-105
	8	21-30	25.5	25	10.5	16	471	593	452	-122
	9	24-33	28.5	26.4	11	15.2	497	622	429	-111
	10	27-36	31.5	26.6	10.4	16	501	588	452	-108
	11	30-39	34.5	26.3	10.7	15.5	495	605	438	-111
	12	33-42	37.5	25.4	10.9	14.8	479	616	418	-116
	13	36-45	40.5	25.3	11	14.2	477	622	401	-114
6	1	1-9	4.5	16	2.8	13.8	301	158	390	-82
	2	18-27	22.5	16.3	3.6	13.8	307	203	390	-93
	3	21-30	25.5	17	4.0	13.6	320	226	384	-91

TRAVERSE	S/No.	DISTANCE MEASURED ALONG TRAVERSE	MID POINT OF MEASURED DISTANCE	R^{α}	R^{β}	R^{γ}	ρ^{α}	ρ^{β}	ρ^{γ}	PERCENTAGE RESIDUAL RESISTIVITY
7	1	1-9m	4.5	17.2	4	13.7	324	226	387	-89
	2	18-27	22.5	19	4.8	13.5	358	271	382	-82
	3	21-30	25.5	21	6.9	12.8	396	390	362	-90
8	1	1-9	4.5	17.6	5.7	9.1	332	322	257	-74
	2	3-12	7.5	13.2	4.3	9	249	243	254	-100
	3	6-15	10.5	12.9	10.3	8	243	582	226	-233
	4	9-18	13.5	12.9	3.7	8.5	243	209	240	-84
	5	12-21	16.5	16.98	2.4	10.7	320	136	302	-36
	6	15-24	19.5	13.3	5	8.8	251	283	249	-112
	7	18-27	22.5	10.9	2.3	3	205	130	85	-5
	8	21-30	25.5	14	10.1	8.2	264	571	232	-204
	9	24-33	28.5	12.8	10.9	7.9	241	616	223	-248
	10	27-36	31.5	13.9	11.3	8.7	262	639	256	-238
	11	30-39	34.5	18.57	4.3	10.61	300	243	300	-81
	12	33.42	37.5	21.23	4	12.03	340	226	340	-66
	13	36.45	40.5	20.16	4.8	11.32	320	271	320	-84

TRAVERSE	S/No.	DISTANCE MEASURED ALONG TRAVERSE	MID POINT OF MEASURED DISTANCE	R^{α}	R^{β}	R^{γ}	ρ^{α}	ρ^{β}	ρ^{γ}	PERCENTAGE RESIDUAL RESISTIVITY
9	1	1-9	4.5	17.1	6.5	13.4	322	367	379	-132
10	1	1-9	4.5	31.7	6.7	20	597	379	565	-58
11	1	1-9	4.5	23.1	8.7	15.5	435	492	438	-114
12	1	1-9	4.5	31.4	11.8	23.0	592	666	649	-122
13	1	1-9	4.5	20.8	6.9	13.6	392	390	384	-97
14	1	1-9	4.5	8.8	6.1	0.7	166	345	20	-120
15	1	1-9	4.5	21.76	2.7	15.21	410	153	430	-42
16	1	1-9	4.5	16.8	4.3	12.8	317	243	362	-91
17	1	1-9	4.5	17.3	3.6	13.5	326	203	382	-79
18	1	1-9	4.5	16.9	4.4	13.1	318	249	370	-95
19	1	1-9	4.5	13.6	9	3.4	256	509	96	-136
	2	3-12	7.5	13	4.9	8.2	245	277	232	-108
	3	6-15	10.5	16.45	3.6	9.9	310	203	280	-55
	4	9-18	13.5	9.7	1.9	7.4	183	107	209	-73
	5	27-36	31.5	12.6	5.4	7	237	305	198	-112
	6	30-39	34.5	13	5.2	8	245	294	226	-112
	7	33-42	37.5	12.9	4.3	8.4	243	243	237	-98
	8	36-45	40.5	11.4	10	10.5	215	565	297	-300

TRAVERSE	S/No.	DISTANCE MEASURED ALONG TRAVERSE	MID POINT OF MEASURED DISTANCE	R^{α}	R^{β}	R^{γ}	ρ^{α}	ρ^{β}	ρ^{γ}	PERCENTAGE RESIDUAL RESISTIVIT
20	1	1-9	4.5	11.6	3.6	7.9	219	203	223	-95
	2	3-12	7.5	13.2	5	8.2	249	282	232	-106
	3	6-15	10.5	15.1	7.5	8.5	284	433	240	-137
	4	9-18	13.5	12.6	5.1	7.2	237	288	203	-107
	5	12-21	16.5	13.2	5	8	249	282	226	-104
	6	15-24	19.5	14.1	5.9	8.1	266	333	228	-111
	7	18-27	22.5	13	4.9	7.9	245	277	223	-104
	8	21-30	25.5	12.8	4.3	8.4	241	243	237	-99
	9	24-33	28.5	11.9	3.8	6.9	224	215	195	-88
	10	27-36	31.5	13.1	6.0	6.8	247	339	192	-115
	11	30-39	34.5	12.9	3.9	8.4	243	220	237	-88
	12	33-42	37.5	14.1	5.3	9.2	266	300	260	-111
	13	36-45	40.5	14.2	5.0	9.6	268	282	271	-106

TRAVERSE	S/No.	DISTANCE MEASURED ALONG TRAVERSE	MID POINT OF MEASURED DISTANCE	R^{α}	R^{β}	R^{γ}	ρ^{α}	ρ^{β}	ρ^{γ}	PERCENTAGE RESIDUAL RESISTIVITY
21	1	1-9	4.5	43.7	9.5	20	823	537	565	-34
	2	3-12	7.5	23	9.8	14	433	554	396	-119
	3	6-15	10.5	22.6	8.3	13.5	426	469	382	-100
	4	9-18	13.5	20	8.5	12	377	480	339	-117
	5	12-21	16.5	21.9	8.0	13	413	452	367	-98
	6	15-24	19.5	22.2	9.8	12.6	418	554	356	-118
	7	18-27	22.5	26	18.6	16.98	490	1051	480	-212
	8	21-30	25.5	24	10.1	13.3	452	599	376	-116
	9	24-33	28.5	20.3	7.5	14.2	382	424	401	-116
	10	27-36	31.5	23.5	8.0	14.5	443	452	410	-95
	11	30-39	34.5	24	8.3	14.8	452	469	418	-96
	12	33-42	37.5	23.6	8.8	15	445	497	424	-107
	13	36-45	40.5	22.1	7.3	15.4	416	413	435	-104

TRAVERSE	S/No.	DISTANCE MEASURED ALONG TRAVERSE	MID POINT OF MEASURED DISTANCE	R^{α}	R^{β}	R^{γ}	ρ^{α}	ρ^{β}	ρ^{γ}	PERCENTAGE RESIDUAL RESISTIVITY
22	1	1-9	4.5	23.1	8	15	435	452	424	-101
	2	3-12	7.5	21.4	7.3	14	403	413	396	-101
	3	6-15	10.5	22.2	7.9	14.9	418	447	421	-108
	4	9-18	13.5	23	8.0	14.8	433	452	418	-101
	5	12-21	16.5	20.9	7	13	394	395	367	-93
	6	15-24	19.5	21.2	7.2	14.3	399	420	404	-101
	7	18-27	22.5	22.29	9.8	16.2	420	554	458	-106
	8	21-30	25.5	23.6	8.7	15	445	492	424	-106
	9	24-33	28.5	24	9.3	15.4	452	526	435	-113
	10	27-36	31.5	20.9	7.3	13	394	413	367	-98
	11	30-39	34.5	21.6	8.2	12.9	407	463	365	-103
	12	33-42	37.5	22.6	8.8	14	426	497	396	-110
	13	36-45	40.5	24.2	9.6	14.5	456	542	410	-109

TRAVERSE	S/No.	DISTANCE MEASURED ALONG TRAVERSE	MID POINT OF MEASURED DISTANCE	R^{α}	R^{β}	R^{γ}	ρ^{α}	ρ^{β}	ρ^{γ}	PERCENTAGE RESIDUAL RESISTIVITY
23	1	1-9	4.5	26.7	7	19.5	503	395	551	-88
	2	3-12	7.5	31.4	6.3	24.8	592	356	701	-79
	3	6-15	10.5	27	7.3	20	509	413	565	-92
	4	9-18	13.5	31.6	6.2	25.2	595	350	712	-78
	5	12-21	16.5	30	7.2	23.2	565	407	656	-88
	6	15-24	19.5	26.5	6.2	20.1	499	350	568	-84
	7	18-27	22.5	27.5	6.0	21.2	518	339	599	-81
	8	21-30	25.5	24	4.4	19.6	452	249	554	-78
	9	24-33	28.5	25.1	8.9	16.4	473	503	463	-104
	10	27-36	31.5	21.2	5.4	15.3	399	305	432	-85
	11	30-39	34.5	21.8	5.7	16	411	322	452	-88
	12	33-42	37.5	22.6	4.0	18.5	426	326	523	-99

TRAVERSE	S/No.	DISTANCE MEASURED ALONG TRAVERSE	MID POINT OF MEASURED DISTANCE	R^{α}	R^{β}	R^{γ}	ρ^{α}	ρ^{β}	ρ^{γ}	PERCENTAGE RESIDUAL RESISTIVITY
24	1	1-9	4.5	23.2	7	15.5	437	395	438	-91
	2	3-12	7.5	24.1	8.7	15	454	491	424	-102
	3	6-15	10.5	21.2	6.5	14.9	399	367	421	-97
	4	9-18	13.5	17.6	3.5	14.6	332	198	413	-84
	5	12-21	16.5	18.4	4	13.8	346	226	390	-78
	6	15-24	19.5	19.2	4.5	15.1	362	254	427	-88
	7	18-27	22.5	20.6	6	14.8	388	339	418	-95
	8	21-30	25.5	20.1	5.2	15	379	294	424	-89
	9	24-33	28.5	21.5	6	15.3	405	339	432	-90

TRAVERSE	S/No.	DISTANCE MEASURED ALONG TRAVERSE	MID POINT OF MEASURED DISTANCE	R^{α}	R^{β}	R^{γ}	ρ^{α}	ρ^{β}	ρ^{γ}	PERCENTAGE RESIDUAL RESISTIVITY
25	1	1-9	4.5	20.1	4.8	15	377	271	424	-84
	2	3-12	7.5	18.2	3.9	14.6	343	220	413	-85
	3	6-15	10.5	17.3	4	14	326	226	396	-91
	4	9-18	13.5	16.8	3.5	13.8	317	198	390	-85
	5	12-21	16.5	16.4	3.5	13.4	309	198	379	-87
	6	15-24	19.5	22.5	5	12.73	424	283	360	-82
	7	18-27	22.5	20.1	5.1	15	377	288	424	-80
	8	21-30	25.5	18	5.9	14.3	339	333	401	-117
	9	24-33	28.5	21.3	6.3	15.4	401	356	435	-97
	10	27-36	31.5	22.6	6.9	15.2	426	390	430	-92
	11	30-39	34.5	24.1	6.6	10.6	454	373	300	-95
	12	33-42	37.5	23.2	5.0	11.32	437	283	320	-83
	13	36-45	40.5	19.7	5.0	15.6	371	283	441	-95